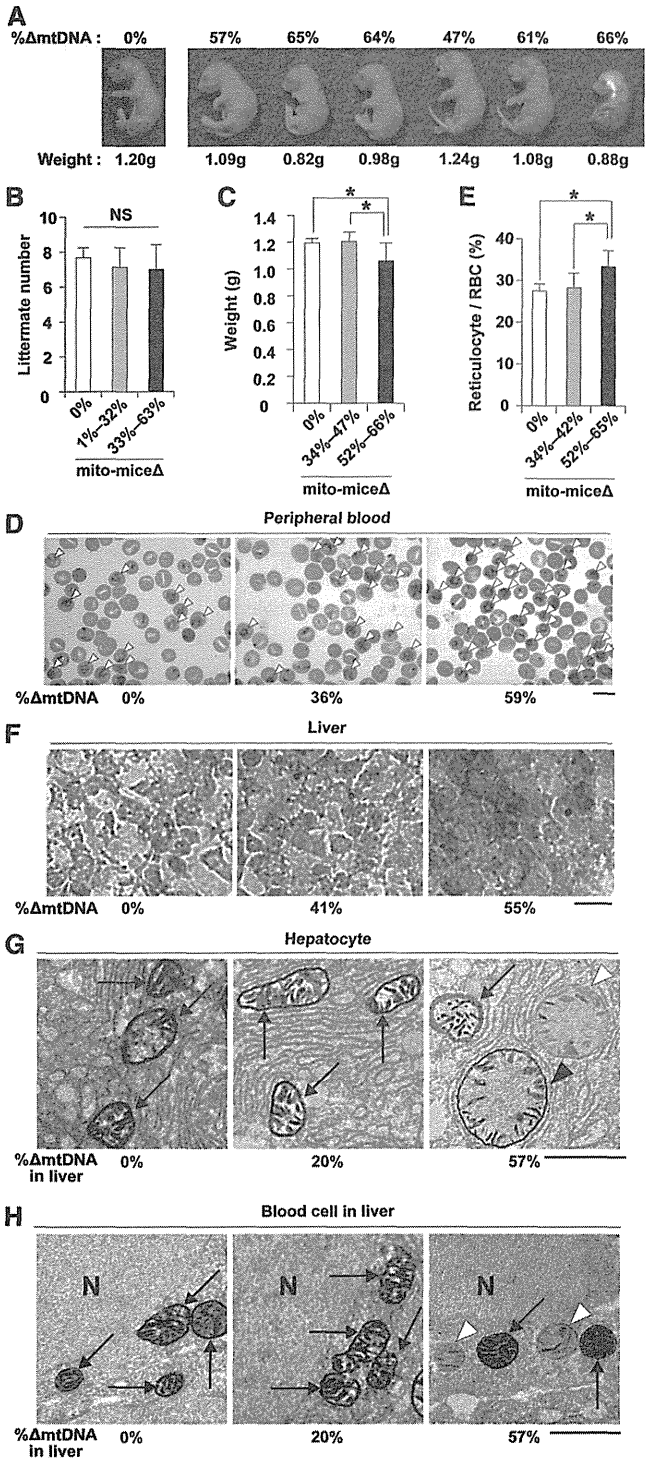

Figure 3 Phenotypic observations of late-stage embryos of mito-miceΔ. All embryos were obtained at embryonic day 18.5. (A) Morphological observation of late-stage embryos carrying 0–66% ΔmtDNA in their tails, as indicated. The embryo carrying no ΔmtDNA (left side) was a wild-type B6 control. The six embryos carrying ΔmtDNA were obtained from a single mother. The weight of each embryo is shown below the panel. (B) Comparison of littermate number. Average numbers of littermates from mothers carrying 0% (white), 1–32% (gray), or 33–63% (black) ΔmtDNA. Data are presented as mean ± SD. NS, not significant. (C) Relationship between weight and ΔmtDNA load in late-stage embryos carrying 0% (white), 34–47% (gray), or 52–66% (black) ΔmtDNA. Data are presented as mean ± SD. Asterisks indicate significant differences ($P < 0.05$). (D) Cytological observation of peripheral blood samples from late-stage embryos. Peripheral blood samples carrying 0%, 36%, and 59% ΔmtDNA, respectively, were stained with new methylene blue. In this method, reticulocytes, a type of immature red blood cells (RBC), are visualized as cells with blue inclusions (open arrowheads). Scale bar, 10 μm. (E) Average proportion of reticulocytes in total RBCs in peripheral blood samples from late-stage embryos carrying 0% (white), 34–42% (gray), or 52–65% (black) ΔmtDNA. Data are presented as mean ± SD. Asterisks indicate significant differences ($P < 0.05$). (F) Histologic observations of iron metabolism in liver samples from late-stage embryos. Liver samples carrying 0%, 41%, and 55% ΔmtDNA, respectively, were stained with Prussian blue. In this method, abnormal iron metabolism is visualized as blue deposits. Scale bar, 10 μm. (G) and (H) Electron microscopic observation of COX activity in liver samples from late-stage embryos. Mitochondria in hepatocytes and blood cells are shown as (G) and (H), respectively. Arrows indicate mitochondria that appeared normal in shape and COX activity, open arrowheads indicate COX-deficient mitochondria, and the closed arrowheads indicate swollen mitochondria with COX activity. N, nucleus. Scale bar, 1 μm.

their tails. We also examined 55 E18.5 embryos from wild-type B6 mice as a normal control. None of the E18.5 embryos of wild-type B6 mice showed lethal phenotypes. Among the E18.5 embryos from mito-miceΔ, three (5.5%) showed lethal phenotypes, and their tails carried 66%, 67%, and 70% ΔmtDNA, respectively, indicating that embryonic lethal phenotypes were restricted to embryos carrying a high load of ΔmtDNA. A typical example of an embryo with a lethal phenotype is shown in Figure 3A (right side): the embryo was atrophied and discolored when compared with littermate embryos carrying <66% ΔmtDNA in their tails. However, there was no significant difference in littermate number between normal mice and mito-miceΔ at E18.5 (Figure 3B). Thus, we concluded that the embryonic lethality was a rare event that was difficult to relate to the observation of frequent early death in mito-miceΔ.

We then examined the relationship between body weight and ΔmtDNA load in tails (Figure 3, A and C). The average body weight of wild-type E18.5 embryos was 1.19 ± 0.03 g ($n = 7$), and that of E18.5 embryos carrying 34–47% ΔmtDNA (1.20 ± 0.07 g, $n = 8$) was in the normal range. In contrast, a substantially lower body weight was seen in E18.5 embryos carrying 52–66% ΔmtDNA (1.05 ± 0.13 g, $n = 14$, $P < 0.05$). Thus, growth retardation was induced preferentially in E18.5 embryos carrying ≥50% ΔmtDNA loads in tails, which was associated with frequent early death after birth. It is well known that ΔmtDNA is a genetic candidate for involvement in the pathogenesis of PS, which is a rapidly fatal disorder of infancy characterized mainly by sideroblastic anemia (DiMauro and Garone. 2011). Our results suggested the possibility that neonates carrying ≥50% ΔmtDNA may show clinical phenotypes of PS. We therefore examined whether E18.5 embryos carrying ≥50% ΔmtDNA showed sideroblastic anemia. Typical sideroblasts were not observed in peripheral blood samples from E18.5 embryos carrying ≥50% ΔmtDNA. In contrast, compared with normal E18.5 embryos, the number of reticulocytes in peripheral blood samples from E18.5 embryos carrying ≥52% ΔmtDNA showed a statistically significant increase (Figure 3, D and E; $P < 0.05$), although the increase was slight. The proportion of reticulocytes in peripheral blood samples from E18.5 embryos carrying ≤42% ΔmtDNA was similar to that in samples from normal E18.5 embryos (Figure 3, D and E). These data suggested abnormalities of hematopoiesis and the resultant onset of mild anemia in E18.5 embryos carrying ≥50% ΔmtDNA. Because abnormal iron metabolism

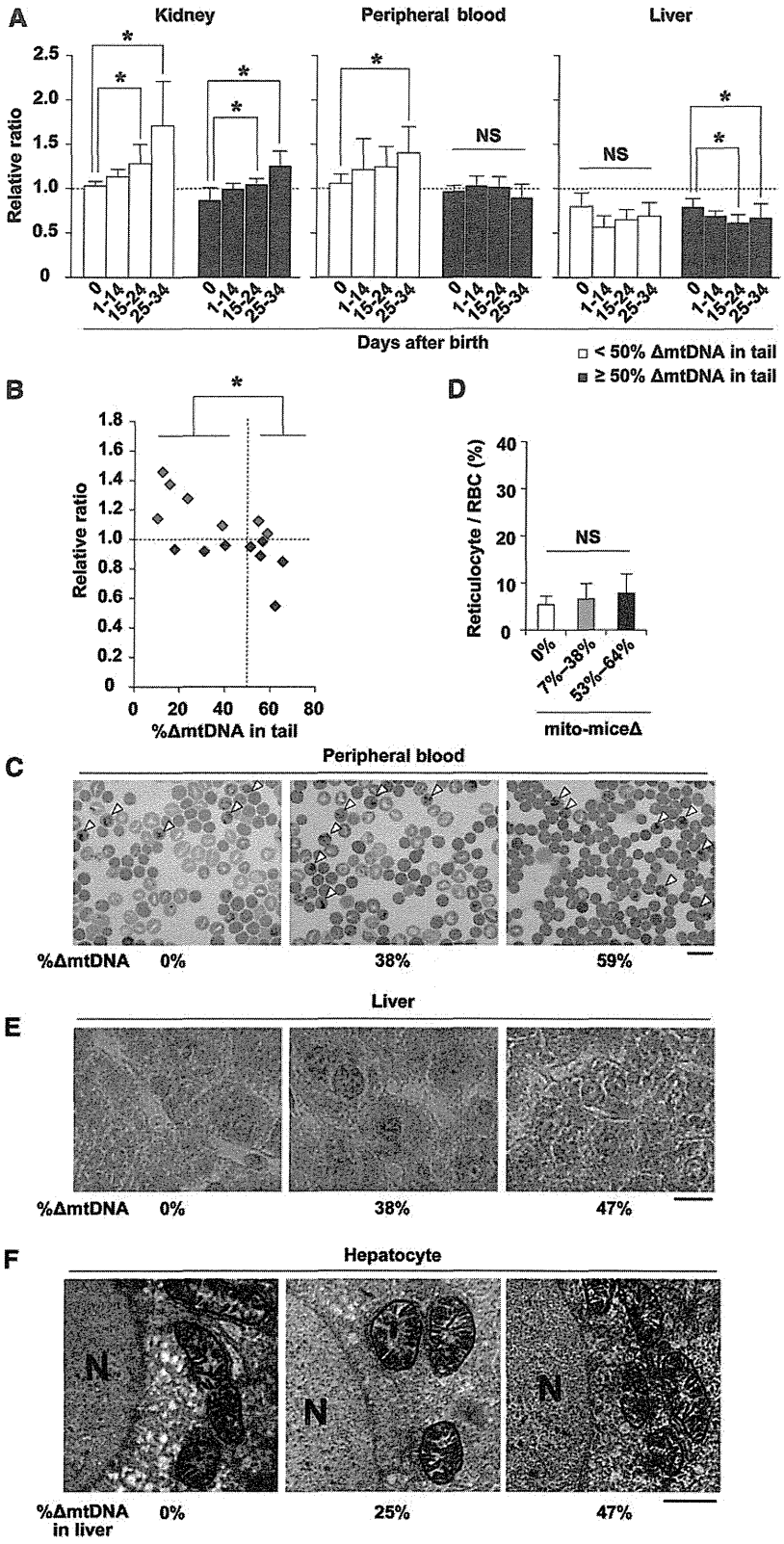

Figure 4 Dynamics of the proportion of ΔmtDNA in early life and phenotypic observations of mito-miceΔ. (A) Dynamics of proportion of ΔmtDNA in affected (peripheral blood and liver) and nonaffected (kidney) tissues at various time points up to and including day 34 after birth. White and black bars indicate populations of mito-miceΔ carrying <50% and ≥50% ΔmtDNA in tail samples, respectively. The relative ratio is the proportion of ΔmtDNA in the tissue tested relative to that in the tail of the same individual at day 0 after birth. Data are presented as mean ± SD. Asterisks indicate significant differences ($P < 0.05$). NS, not significant. (B) Dynamics of the proportion of ΔmtDNA in peripheral blood samples from single individuals during early life. Red and blue symbols indicate cases where the proportion of ΔmtDNA in peripheral blood samples increased and decreased, respectively, between days 14 and 34 after birth. Asterisk indicates significant differences ($P < 0.05$). (C) Cytological observations of peripheral blood samples obtained from mito-miceΔ at day 34 after birth. Peripheral blood samples carrying 0%, 38%, and 59% ΔmtDNA, respectively, were stained with new methylene blue and reticulocytes (open arrowheads) are visualized similar to Figure 3D. Scale bar, 10 μm. (D) Average proportion of reticulocytes in total RBC. Results for peripheral blood samples obtained from mito-miceΔ carrying 0%, 7–38%, and 53–64% ΔmtDNA are shown as white, gray, and black colors, respectively. Data are presented as mean ± SD. NS, not significant. (E) Histologic observations of iron metabolism in liver samples from mito-miceΔ at day 34 after birth. Liver samples carrying 0%, 38%, and 47% ΔmtDNA, respectively, were stained with Prussian blue. Scale bar, 10 μm. (F) COX-EM of liver samples obtained from mito-miceΔ at day 34 after birth. The COX-EM of liver samples carrying 0%, 25%, and 47% ΔmtDNA, respectively, are shown. The loading of 47% ΔmtDNA was the maximum in the liver samples that we examined at day 34, because the proportion of ΔmtDNA in liver was lower than that in tissues during early life. N, nucleus. Bar, 2 μm.

in liver is observed in cases of sideroblastic anemia and PS (Camaschella. 2008; Gurgey *et al.* 1996), we examined pathologic changes in liver samples from E18.5 embryos carrying ΔmtDNA. Deposits of ferric iron indicating abnormal iron metabolism were preferentially observed in liver samples from E18.5 embryos with an increased number of reticulocytes (Figure 3F). On the basis of these observations, we concluded that ≥50% ΔmtDNA loads could cause PS-like phenotypes in late-stage mouse embryos, although it was not a typical PS.

In our previous studies using mito-miceΔ, accumulation of approximately 70–80% ΔmtDNA loads in various tissues was necessary

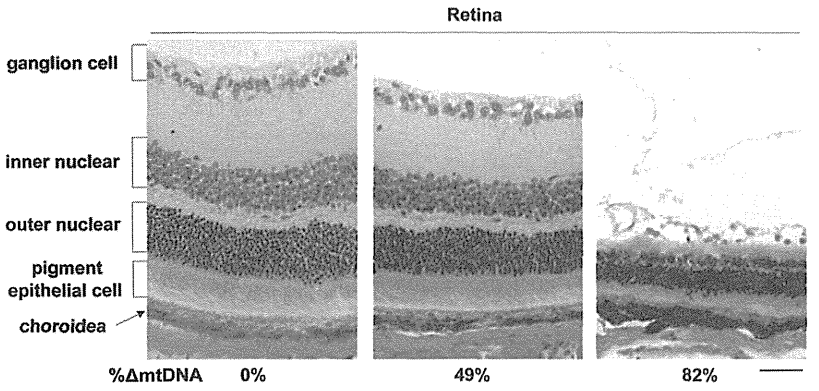

Figure 5 Phenotypic observations of middle-aged mito-miceΔ. Histological observations of retina from mito-miceΔ assayed at 6 months of age. Sections of eye samples were stained with hematoxylin and eosin. The proportion of ΔmtDNA in eye samples from the opposite side is indicated under the each picture. Scale bar, 50 μm.

to induce mitochondrial respiration defects, such as deficiencies of complex IV (COX) in mitochondrial respiratory chains, and the resultant onset of various clinical phenotypes. In contrast, E18.5 embryos showed clinical phenotypes, even when they carried ≥50% ΔmtDNA. These results were expected that threshold for tolerance to accumulation of ΔmtDNA in embryonic liver and blood cells would be lower than that in other tissues. Because electron microscopic observations of COX activity (COX-EM) can visualize COX activity in individual mitochondria of single cells (Nakada *et al.* 2001; Seligman *et al.* 1968), we next performed COX-EM with liver samples from E18.5 embryos carrying various loads of ΔmtDNA. In liver samples carrying ≥50% ΔmtDNA, we observed three types of mitochondria in a single cytoplasm of hepatocytes, mitochondrion that appeared normal in COX activity (arrows in Figure 3G), a swollen mitochondrion with COX activity (closed arrowhead in Figure 3G), and a COX-deficient swollen mitochondrion (open arrowhead in Figure 3G). In blood cells of liver samples carrying ≥50% ΔmtDNA, heterogeneity of COX activity within individual mitochondria was clearly visible (Figure 3H), although swollen mitochondria were not observed. These observations indicated that ≥50% ΔmtDNA loads could induce mitochondrial respiration defects in hepatocytes and blood cells of late-stage embryos. In addition, there were no autophagic ultra-structures around abnormal mitochondria in hepatocytes or blood cells (Figure 3, G and H), indicating that that the COX-deficient mitochondria were not eliminated by the mitophagy, even when a single cytoplasm contained mitochondria with different mitochondrial respiratory functions.

Changes of ΔmtDNA load and clinical phenotypes in mito-miceΔ during early life

The results of the early life span assay described previously (see Figure 1E) clearly showed that there were two populations of neonates carrying ≥50% ΔmtDNA in their tail; the first population showed death phenotypes in the first month after birth, probably due to PS-like phenotypes; and the second population was able to escape early death. In mito-miceΔ, genetic variation is restricted to the load of ΔmtDNA in various tissues, so that phenotypes are strictly induced by the load of ΔmtDNA in affected tissues. Considering the point, there was a possibility that that the ΔmtDNA load decreased preferentially in the peripheral blood and liver of surviving neonates by around 1-month after birth. To test this possibility, we examined ΔmtDNA load in affected and nonaffected tissues of surviving neonates at various time points up to and including day 34 after birth (Figure 4A). In this assay, we could not trace the proportion of ΔmtDNA load in tissues from single neonates, because we had to kill neonates to obtain tissue samples. Thus, we estimated the proportion of ΔmtDNA in each sample relative to that in the tail sample taken on day 0 after birth from the same subject. The animals were analyzed as two subgroups defined by the ΔmtDNA load in the tail (*i.e.*, <50% and ≥50% ΔmtDNA). In kidney samples as a nonaffected tissue, the relative ratios increased with time in both subgroups, suggesting that the proportion of ΔmtDNA in the nonaffected tissues increased independently of the ΔmtDNA load (Figure 4A, $P < 0.05$). In peripheral blood, there were two distinct patterns dependent on ΔmtDNA load. In neonates carrying <50% ΔmtDNA in their tails at day 0, the relative ratios increased with time and the pattern was similar to that of kidney samples ($P < 0.05$). In neonates carrying ≥50% ΔmtDNA in their tails at day 0, the relative ratios in peripheral blood samples did not increase with time. The relative ratios in liver samples from both subgroups did not increase with time. In the case of liver samples from E18.5 embryos carrying ≥50% ΔmtDNA, however, a significant decrease of relative ratios was observed ($P < 0.05$).

To confirm changes in ΔmtDNA load in peripheral blood within same individuals, we collected peripheral blood samples from single neonates carrying 7–64% ΔmtDNA, respectively, in their tails at day 0. We calculated the proportion of ΔmtDNA in peripheral blood on day 34 after birth relative to that on day 14 after birth (Figure 4B). The relative ratios in surviving neonates carrying <50% ΔmtDNA in their tails were >1 and particularly high in neonates carrying <20% ΔmtDNA in their tails. In contrast, neonates carrying ≥50% ΔmtDNA in their tails showed relative ratios <1. There was a significant difference between neonates carrying <50% and ≥50% ΔmtDNA in their tails ($P < 0.05$). These data indicate that the proportion of ΔmtDNA in peripheral blood decreased at an early age (*i.e.*, from days 14 to 34) when the proportion of ΔmtDNA in peripheral blood was ≥50%.

Consistent with these results, abnormalities observed in peripheral blood and liver samples of late-stage embryos (Figure 3, D–G) were not detected on day 34 after birth (Figure 4, C–F). There was no significant difference in reticulocyte number between wild-type mice and mito-miceΔ (Figure 4, C and D). Iron deposits that were seen in livers from late stage embryos carrying ≥50% ΔmtDNA were not observed in the livers carrying 47% ΔmtDNA, which was the maximum proportion of ΔmtDNA observed on day 34 after birth (Figure 4E) because of the decreased ΔmtDNA loads in liver. In COX-EM, abnormalities were not observed in liver samples (Figure 4F). These findings indicate that the decrease of ΔmtDNA loading proportion in peripheral blood and liver of neonates carrying ≥50% ΔmtDNA would be one reason for recovering from PS-like phenotypes and for the resultant survival.

Disease phenotypes of surviving neonates when they reach middle life

At 6 months of age or later, all the surviving mito-miceΔ showed lactic acidosis, heart block, renal failure, male infertility, deafness, and

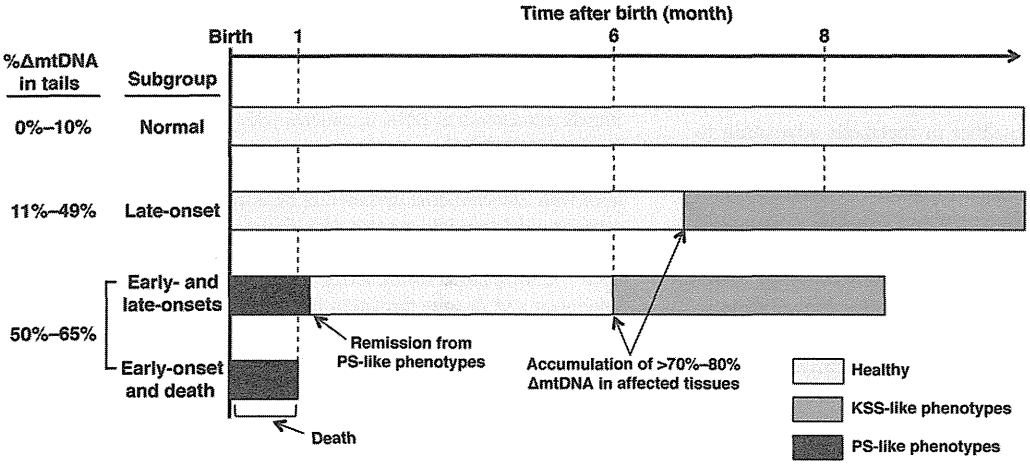

Figure 6 Schematic representation of disease phenotypes in mito-miceΔ population. "Normal" and "late-onset" subgroups in mito-miceΔ population and their clinical features have already been reported as our previous studies (Inoue *et al.* 2000; Nakada *et al.* 2001, 2004, 2006; Ogasawara *et al.* 2010; Tanaka *et al.* 2008). The novelty of this study was to found out two subgroups, "early-onset and death" and "early- and late-onsets" in addition of conventional two subgroups, "normal" and "late-onset" subgroups.

abnormalities in long-term memory as reported previously, when the proportion of ΔmtDNA in affected tissues reached approximately 70–80% (Inoue *et al.* 2000; Nakada *et al.* 2001, 2004, 2006; Ogasawara *et al.* 2010; Tanaka *et al.* 2008). In some of surviving mito-miceΔ carrying >80% ΔmtDNA, retinal abnormalities were observed (Figure 5). These results indicated that neonates that remitted from PS-like phenotypes in early life expressed KSS-like phenotypes in their middle life.

DISCUSSION

Taking the current results together with our previous ones, we summarized the development of mitochondrial diseases in mito-miceΔ (Figure 6). On the basis of the difference in ΔmtDNA loads and the resultant mitochondrial disease phenotypes, mito-miceΔ population is classified into four subgroups. The first subgroup was mito-miceΔ carrying ≤10% ΔmtDNA at the birth. They showed normal phenotypes because ΔmtDNA loads did not reach >70–80% in various tissues through the life (Normal subgroup in Figure 6). The second subgroup was mito-miceΔ carrying 11–49% ΔmtDNA just after birth, and the mice appeared healthy until middle age (6 months) or later, but when the ΔmtDNA load reached >70–80% in various tissues, they expressed KSS-like phenotypes (late-onset subgroup in Figure 6). The main clinical features in this subgroup, such as low body weight, lactic acidosis, heart block, renal failure, deafness, male infertility, and abnormal long-term memory, has been reported previously (Inoue *et al.* 2000; Nakada *et al.* 2001, 2004, 2006; Ogasawara *et al.* 2010; Tanaka *et al.* 2008). The third and fourth subgroups were mito-miceΔ carrying ≥50% ΔmtDNA just after birth. When the ΔmtDNA load in late-stage embryos reached ≥50%, abnormalities of hematopoiesis and iron metabolisms in liver were induced, thus leading to PS-like phenotypes (*i.e.*, abnormalities in hematopoiesis and iron metabolism; Figure 3, D–F), although >70–80% ΔmtDNA loads were necessary for the onset of KSS-like phenotypes in adult mito-miceΔ. Half of those expressing PS-like phenotypes died in early life (≤34 days after birth). The third subgroup, therefore, was the case of onset of PS-like phenotypes and the resultant early death (early-onset and death subgroup in Figure 6). The rest escaped from the early death, because PS-like phenotypes in them disappeared consistent with a decrease of ΔmtDNA load in affected tissues (see Figure 4, D and E for the cases of peripheral blood and liver samples, respectively). However, they expressed KSS-like phenotypes, when ΔmtDNA load reached >70–80% in affected tissues (Figure 5). Thus, the fourth subgroup was the case of transient onsets of PS-like and KSS-like phenotypes in early and middle age, respectively, in a single mito-miceΔ (Early-and late-onsets subgroup in Figure 6).

Heterogeneous distribution of mitochondria with and without COX activity in single cells would be important for elucidating the reason why the pathogenic threshold load of ΔmtDNA in embryonic blood and liver was lower than that in other tissues. We have previously reported that a uniform distribution of mitochondria either with or without COX activity occurs in somatic cells of adult mito-miceΔ, irrespective of whether the tissues contain low or high loads of ΔmtDNA (Nakada *et al.* 2001). This finding indicates the occurrence of mitochondrial genetic complementation in which individual mitochondria exchange gene products derived from mtDNA through their fusion and fission. Because mitochondria carrying ΔmtDNA can be supplied by mitochondria carrying wild-type mDNA, tissues carrying ΔmtDNA did not show mitochondrial respiration defects until ΔmtDNA accumulated to a level of >70–80%. In contrast, here we observed that blood cells and hepatocytes in late-stage embryos showing PS-like phenotypes contained mitochondria with heterogeneous ultrastructures and COX activity levels (Figure 3, G and H). This finding suggested the existence of deficiencies of mitochondrial fusion or fission or both, and a lack of mitochondrial genetic complementation in these late-stage embryonic cells. Such deficiencies could be one reason that a load of ≥50% ΔmtDNA could cause pathogenicity in blood cells and hepatocytes of late-stage embryos, whereas a higher load is required in adult mice. Moreover, it has been reported that mitochondrial dynamics, a continuous mitochondrial fusion and fission, is necessary to maintain normal mitochondrial respiratory function in mammals (Chen *et al.* 2010; Ishihara *et al.* 2009). Therefore, it is possible that deficiencies of mitochondrial dynamics and genetic complementation in embryonic blood cells and hepatocytes enhance the pathogenicity of ΔmtDNA in the case of a ≥50% ΔmtDNA load.

PS-like phenotypes induced by the abnormalities of hematopoiesis and iron metabolisms in livers of late-stage embryos carrying ≥50% ΔmtDNA were the main clinical features, but it is unclear why a half of the neonates carrying ≥50% ΔmtDNA died early. There are several possible explanations for this phenomenon. The first is that the pups might have suffered acute oxidative stress because newborns and infants are particularly prone to oxidative stress (Saugstad 2005). Newborns and infants have reduced antioxidant defense mechanisms as well as high levels of free iron, which are required for the Fenton reaction (Saugstad 2005); approximately 20% neonates died on day 1 after birth even in wild-type B6 mice (Figure 1, B and C). Because neonates

carrying ≥50% ΔmtDNA in their tails possessed iron deposits in liver (Figure 3F), the high level of iron could promote the Fenton reaction, resulting in additional oxidative stress when the neonates are exposed to a high oxygen concentration after delivery (Singer and Muhlfeld 2007). Another possibility was that abnormalities in metabolic adaptation to the aerobic condition just after birth might cause frequent early death in mito-miceΔ. Anaerobic glycolysis is the major source of cellular ATP in fetal tissues. In cells with mitochondrial respiration defects as the result of pathogenic mutant mtDNAs, glycolysis is enhanced as a compensatory mechanism to maintain ATP levels. Therefore, ΔmtDNA might not demonstrate its pathogenicity in various cells during embryogenesis. Supporting this notion, we observed only rare incidents of embryonic lethality in mito-miceΔ. After birth, neonates carrying ΔmtDNA have to change from anaerobic to aerobic energy metabolism in various cells as soon as possible, but they would find this process difficult due to their systemic and chronic mitochondrial respiration defects.

In summary, our model mouse study showed that a single ΔmtDNA molecule has a pathogenic potential to cause PS-like and KSS-like phenotypes at early and middle life, respectively, and also suggested that difference in threshold for tolerance to accumulation of ΔmtDNA in affected tissues between young infants and adults was a possible reason for the onset of disease phenotypes in mito-miceΔ. In addition, dynamics of ΔmtDNA load in affected tissues well correlated with the transition of disease phenotypes in mito-miceΔ. At this sage, we considered that decreased proportion of ΔmtDNA in peripheral blood and liver from young infants carrying >50% ΔmtDNA was important to recover from PS-like phenotypes. However, we could not rule out a possibility that the decreased proportion of ΔmtDNA in affected tissues was a result by which young infants carrying >50% ΔmtDNA recovered from PS-like phenotypes. Therefore, biological and clinical significance of ΔmtDNA dynamics associating with changes of disease phenotypes remains to be answered.

ACKNOWLEDGMENTS

This work was supported by a Grant-in-Aid for Scientific Research (A) (No. 23240058 and No. 25250011) from the Ministry of Education, Culture, Sports, Science and Technology of Japan (MEXT) to K.N. and J.I.H.; by a Grant-in-Aid for Challenging Exploratory Research (No. 22650091) from MEXT to K.N.; and by a Grant-in-Aid for Scientific Research on Innovative Areas (No. 24117503) from Japan Society for the Promotion of Science to J.I.H. This work was also supported by Grants-in-Aid of the Research on Intractable Diseases (Mitochondrial Disorder) from the Ministry of Health, Labor and Welfare of Japan to K.N.

LITERATURE CITED

Camaschella, C., 2008 Recent advances in the understanding of inherited sideroblastic anaemia. Br. J. Haematol. 143: 27–38.

Chen, H., M. Vermulst, Y. E. Wang, A. Chomyn, T. A. Prolla *et al.*, 2010 Mitochondrial fusion is required for mtDNA stability in skeletal muscle and tolerance of mtDNA mutations. Cell 141: 280–289.

DiMauro, S., and C. Garone, 2011 Metabolic disorders of fetal life: glycogenoses and mitochondrial defects of the mitochondrial respiratory chain. Semin. Fetal Neonatal Med. 16: 181–189.

Gurgey, A., I. Ozalp, A. Rotig, T. Coskun, G. Tekinalp *et al.*, 1996 A case of Pearson syndrome associated with multiple renal cysts. Pediatr. Nephrol. 10: 637–638.

Holt, I. J., A. E. Harding, and J. A. Morgan-Hughes, 1988 Deletions of muscle mitochondrial DNA in patients with mitochondrial myopathies. Nature 331: 717–719.

Inoue, K., K. Nakada, A. Ogura, K. Isobe, Y. Goto *et al.*, 2000 Generation of mice with mitochondrial dysfunction by introducing mouse mtDNA carrying a deletion into zygotes. Nat. Genet. 26: 176–181.

Ishihara, N., M. Nomura, A. Jofuku, H. Kato, S. O. Suzuki *et al.*, 2009 Mitochondrial fission factor Drp1 is essential for embryonic development and synapse formation in mice. Nat. Cell Biol. 11: 958–966.

Larsson, N. G., and D. A. Clayton, 1995 Molecular genetic aspects of human mitochondrial disorders. Annu. Rev. Genet. 29: 151–178.

Larsson, N. G., E. Holme, B. Kristiansson, A. Oldfors, and M. Tulinius, 1990 Progressive increase of the mutated mitochondrial DNA fraction in Kearns-Sayre syndrome. Pediatr. Res. 28: 131–136.

McFarland, R., K. M. Clark, A. A. Morris, R. W. Taylor, S. Macphail *et al.*, 2002 Multiple neonatal deaths due to a homoplasmic mitochondrial DNA mutation. Nat. Genet. 30: 145–146.

McShane, M. A., S. R. Hammans, M. Sweeney, I. J. Holt, T. J. Beattie *et al.*, 1991 Pearson syndrome and mitochondrial encephalomyopathy in a patient with a deletion of mtDNA. Am. J. Hum. Genet. 48: 39–42.

Nakada, K., K. Inoue, T. Ono, K. Isobe, A. Ogura *et al.*, 2001 Inter-mitochondrial complementation: mitochondria-specific system preventing mice from expression of disease phenotypes by mutant mtDNA. Nat. Med. 7: 934–940.

Nakada, K., A. Sato, H. Sone, A. Kasahara, K. Ikeda *et al.*, 2004 Accumulation of pathogenic DeltamtDNA induced deafness but not diabetic phenotypes in mito-mice. Biochem. Biophys. Res. Commun. 323: 175–184.

Nakada, K., A. Sato, K. Yoshida, T. Morita, H. Tanaka *et al.*, 2006 Mitochondria-related male infertility. Proc. Natl. Acad. Sci. USA 103: 15148–15153.

Ogasawara, E., K. Nakada, and J. Hayashi, 2010 Lactic acidemia in the pathogenesis of mice carrying mitochondrial DNA with a deletion. Hum. Mol. Genet. 19: 3179–3189.

Rotig, A., T. Bourgeron, D. Chretien, P. Rustin, and A. Munnich, 1995 Spectrum of mitochondrial DNA rearrangements in the Pearson marrow-pancreas syndrome. Hum. Mol. Genet. 4: 1327–1330.

Sato, A., K. Nakada, H. Shitara, A. Kasahara, H. Yonekawa *et al.*, 2007 Deletion-mutant mtDNA increases in somatic tissues but decreases in female germ cells with age. Genetics 177: 2031–2037.

Sato, A., T. Kono, K. Nakada, K. Ishikawa, S. Inoue *et al.*, 2005 Gene therapy for progeny of mito-mice carrying pathogenic mtDNA by nuclear transplantation. Proc. Natl. Acad. Sci. USA 102: 16765–16770.

Saugstad, O. D., 2005 Oxidative stress in the newborn—a 30-year perspective. Biol. Neonate 88: 228–236.

Seligman, A. M., M. J. Karnovsky, H. L. Wasserkrug, and J. S. Hanker, 1968 Nondroplet ultrastructural demonstration of cytochrome oxidase activity with a polymerizing osmiophilic reagent, diaminobenzidine (DAB). J. Cell Biol. 38: 1–14.

Singer, D., and C. Muhlfeld, 2007 Perinatal adaptation in mammals: the impact of metabolic rate. Comp. Biochem. Physiol. A Mol. Integr. Physiol. 148: 780–784.

Tanaka, D., K. Nakada, K. Takao, E. Ogasawara, A. Kasahara *et al.*, 2008 Normal mitochondrial respiratory function is essential for spatial remote memory in mice. Mol. Brain 1: 21.

Wallace, D. C., 1999 Mitochondrial diseases in man and mouse. Science 283: 1482–1488.

Communicating editor: D. W. Threadgill

PLOS ONE

Mitochondrial DNA Mutations in Mutator Mice Confer Respiration Defects and B-Cell Lymphoma Development

Takayuki Mito[1], Yoshiaki Kikkawa[2], Akinori Shimizu[1], Osamu Hashizume[1], Shun Katada[1], Hirotake Imanishi[1], Azusa Ota[1], Yukina Kato[1], Kazuto Nakada[1], Jun-Ichi Hayashi[1]*

1 Faculty of Life and Environmental Sciences, University of Tsukuba, Tsukuba, Japan, **2** Mammalian Genetics Project, Tokyo Metropolitan Institute of Medical Science, Tokyo, Japan

Abstract

Mitochondrial DNA (mtDNA) mutator mice are proposed to express premature aging phenotypes including kyphosis and hair loss (alopecia) due to their carrying a nuclear-encoded mtDNA polymerase with a defective proofreading function, which causes accelerated accumulation of random mutations in mtDNA, resulting in expression of respiration defects. On the contrary, transmitochondrial mito-miceΔ carrying mtDNA with a large-scale deletion mutation (ΔmtDNA) also express respiration defects, but not express premature aging phenotypes. Here, we resolved this discrepancy by generating mtDNA mutator mice sharing the same C57BL/6J (B6J) nuclear background with that of mito-miceΔ. Expression patterns of premature aging phenotypes are very close, when we compared between homozygous mtDNA mutator mice carrying a B6J nuclear background and selected mito-miceΔ only carrying predominant amounts of ΔmtDNA, in their expression of significant respiration defects, kyphosis, and a short lifespan, but not the alopecia. Therefore, the apparent discrepancy in the presence and absence of premature aging phenotypes in mtDNA mutator mice and mito-miceΔ, respectively, is partly the result of differences in the nuclear background of mtDNA mutator mice and of the broad range of ΔmtDNA proportions of mito-miceΔ used in previous studies. We also provided direct evidence that mtDNA abnormalities in homozygous mtDNA mutator mice are responsible for respiration defects by demonstrating the co-transfer of mtDNA and respiration defects from mtDNA mutator mice into mtDNA-less (ρ^0) mouse cells. Moreover, heterozygous mtDNA mutator mice had a normal lifespan, but frequently developed B-cell lymphoma, suggesting that the mtDNA abnormalities in heterozygous mutator mice are not sufficient to induce a short lifespan and aging phenotypes, but are able to contribute to the B-cell lymphoma development during their prolonged lifespan.

Citation: Mito T, Kikkawa Y, Shimizu A, Hashizume O, Katada S, et al. (2013) Mitochondrial DNA Mutations in Mutator Mice Confer Respiration Defects and B-Cell Lymphoma Development. PLoS ONE 8(2): e55789. doi:10.1371/journal.pone.0055789

Editor: Yidong Bai, University of Texas Health Science Center at San Antonio, United States of America

Received September 5, 2012; **Accepted** December 31, 2012; **Published** February 13, 2013

Funding: This work was supported by Scientific Research on Innovative Areas 24117503 (to JIH) and Scientific Research A 23240058 (to KN) from Japan Society for the Promotion of Science (JSPS http://www.jsps.go.jp/). The funders had no role in study design, data collection and analysis, decision to publish, or preparation of the manuscript.

Competing Interests: The authors have declared that no competing interests exist.

* E-mail: jih45@biol.tsukuba.ac.jp

Introduction

It has been hypothesized that pathogenic mtDNA mutations that induce significant mitochondrial respiration defects cause mitochondrial diseases [1,2] and could also be involved in aging and age-associated disorders including tumor development [1–5]. This hypothesis is partly supported by studies in mtDNA mutator mice [6–8]: they possess a nuclear-encoded mtDNA polymerase with a defective proofreading function that leads to enhanced accumulation of random mutations in mtDNA with age, and the subsequent phenotypic expression of age-associated respiration defects and premature aging phenotypes, but not tumor development.

On the contrary, our previous studies [9,10] showed that transmitochondrial mito-miceΔ carrying mtDNA with a large-scale deletion mutation (ΔmtDNA) expressed age-associated respiration defects, but not express the premature aging phenotypes. Similar results were obtained in other transmitochondrial mito-miceCOI^{M}, which have an mtDNA point mutation in the *COI* gene [11]. Recently, we generated new transmitochondrial mito-miceND6^{M}, which have an mtDNA point mutation in the *ND6* gene [12] that is derived from Lewis lung carcinomas, and confers respiration defects and overproduction of reactive oxygen species (ROS) [13]. Mito-miceND6^{M} did not express premature aging phenotypes, but were prone to B-cell lymphoma development [14]. Thus, it appears to be discrepant that premature aging phenotypes are exclusively observed in mtDNA mutator mice [6–8], but not in transmitochondrial mito-mice [9–11,14], even though they all express mitochondrial respiration defects caused by mutated mtDNA.

This discrepancy may partly be the result of differences in the nuclear genetic background between mtDNA mutator mice and transmitochondrial mito-mice. It is also possible that the premature aging phenotypes found exclusively in mtDNA mutator mice are not caused by mutations in mtDNA, because inter-mitochondrial interaction and the resultant genetic complementation in mammalian mitochondria may prevent random mutations in mtDNA being expressed as respiration defects [10,15,16].

To clarify these issues, first we generated mtDNA mutator mice with the same C57BL/6J (B6J) nuclear genetic background as that of mito-miceΔ, and examined whether they still expressed respiration defects and premature aging phenotypes. We then

transferred mtDNA from mtDNA mutator mice into mtDNA-less (ρ^0) mouse cells and isolated transmitochondrial cybrids possessing mtDNA transferred from the mtDNA mutator mice, but not possessing defective mtDNA polymerase from the mtDNA mutator mice, and examined whether the resultant transmitochondrial cybrids expressed the expected respiration defects.

Materials and Methods

Mice

Inbred B6J mice generated by sibling mating more than 40 times were obtained from CLEA Japan. Mito-miceΔ were generated in our previous report [9]. Homo- and heterozygous mtDNA mutator mice were generated based on the procedures reported previously [6,7] with a few modifications. We converted nucleotides 4460–4465 of the PolgA sequence from GACCGA to GCGCGC to introduce a D257A mutation in PolgA and create *BssH*II site for genotyping by PCR-RFLP method. Animal experiments were performed in accordance with protocols approved by the Experimental Animal Committee of the University of Tsukuba, Japan (Approval number: 12-295).

Mouse Cell Lines and Cell Culture

Mouse B82 cells are fibrosarcomas derived from the L929 fibroblast cell line (C3H/An mouse strain) [17], and ρ^0 B82 cells without mtDNA were obtained in our previous study [9]. Transmitochondrial cybrids were isolated by the fusion of the platelets from mtDNA mutator mice with ρ^0 B82 cells by polyethylene glycol and subsequent selection that allows exclusive growth of the trans-mitochondrial cybrids (see Table S1). For isolation of immortalized 3T3 cells, MEFs in a 6-cm culture dish at a density of 3×10^5 cells per dish were cultured using the 3T3 protocol [18,19]. Briefly, 3 days after the cells had been plated at 3×10^5 cells per dish, we trypsinized them, counted the total cell numbers, and then replated 3×10^5 cells into 6-cm dishes. These processes were repeated until immortalized cells appeared. The mouse cells and cell lines were grown in DMEM (Sigma) containing 10% fetal calf serum, uridine (50 ng/ml), and pyruvate (0.1 mg/ml).

Estimation of ΔmtDNA Proportion in Mito-Mice

The proportion of wild type mtDNA and ΔmtDNA was determined by a real-time PCR technique, as described previously [20].

Analysis of COX Activity

Histochemical analyses for COX and SDH activity were carried out based on the procedures as described previously [21] using cryosections (10 μm thick) of cardiac muscles and renal tissues, and coverslips with growing 3T3 cells.

Measurement of O_2 Consumption Rates in Mouse Cell Lines

The rate of oxygen consumption was measured by trypsinizing cells, incubating the suspension in PBS, and recording oxygen consumption in a 2.0-ml polarographic cell at 37°C with a Clark-type oxygen electrode (Yellow Springs Instruments).

Analysis of mtDNA Mutations

Total DNA was extracted from cells and tissues, and somatic mtDNA mutation load was determined by PCR, cloning, and sequencing, as described earlier (Ref.), using primers that specifically amplified a part of *COX1* gene (nucleotide pair 6,006–6,522) of mouse mtDNA. PCR products were subcloned into the pTA2 T-vector using by TArget Clone Plus Kit (TOYOBO, Osaka, Japan). Fifty plasmids were randomly selected from the each sample, were isolated using DirectPrep 96 MiniPrep Kit (Qiagen, Valencia, CA) and sequenced with M13 forward and reverse primers using BigDye Terminator Kit (Life Technologies, Grand Island, NY) on an Applied Biosystems 3130xl Genetic Analyzer. Sequences were assembled and edited in GENETYX ver10 (GENETYX Corporation, Tokyo, Japan).

Southern-blot Analysis

Total DNA (5 μg and 3 μg) extracted from cells and tissues was digested with the restriction endonuclease *Xho*I. Restriction fragments were separated in 1.0% agarose gel, transferred to Hybond N^+ membrane (GE Healthcare Lifesciences) and hybridized with alkaline phosphatase-labelled mouse mtDNA probes. Probe-bound alkaline phosphatase was used to catalyse light production by enzymatic decomposition of CDP-Star Detection Reagent (GE Healthcare Lifesciences). Chemiluminescences of fragments were measured with a bioimaging analyser, EZ-Capture ST (ATTO).

Lactate and Glucose Measurement

To determine blood lactate and glucose concentrations, blood was collected from the tail veins of mice. Lactate and glucose concentrations were measured with an automatic blood lactate test meter (Lactate Pro; Arkray) and glucose test meter (Dexter ZII; Bayer), respectively.

Histological Analyses

Formalin-fixed, paraffin-embedded serial sections were used for histological analyses. Hematoxylin and eosin–stained sections were used for histopathological analysis to identify tumor tissues. The immunohistochemical analysis was performed with antibody to CD45 (BD Biosciences) to determine whether the tumor tissues originated from leukocytes, and subsequently with antibodies to B220 (BD Biosciences) and CD3 (Santa Cruz) to determine whether the tumor tissues were of B-cell or T-cell origin, respectively.

Measurement of ROS Production in Mitochondria

ROS generation was detected with the mitochondrial superoxide indicator MitoSOX-Red (Life Technologies). Cells were incubated with 1 μM MitoSOX-Red for 15 min at 37°C in phosphate-buffered saline (PBS), washed twice with PBS, and then immediately analyzed with a FACScan flow cytometer (Becton Dickinson).

Statistical Analysis

Data were analyzed by Dunnett's test or one-way ANOVA followed by Dunnett's post test. Kaplan–Meier curves were assessed with the log-rank test. Values with $P<0.05$ were considered significant.

Results

Mitochondrial Respiration Defects in mtDNA Mutator Mice with a B6J Nuclear Background

We generated heterozygous (+/m) and homozygous (m/m) mtDNA mutator mice with a B6J nuclear background (see Materials and Methods), and examined whether mtDNA mutator mice with a B6J nuclear background also express respiration defects. Young (10-month-old) mice were used for examination of their mitochondrial respiratory function. Age-matched normal B6J

mice and mito-miceΔ with a B6J nuclear background were used as positive and negative controls, respectively. Histochemical analysis of mitochondrial cytochrome *c* oxidase (COX) activity in mouse tissues showed reduced COX activity in homozygous m/m mutator mice and mito-miceΔ, and mild COX defects in heterozygous +/m mutator mice (Fig. 1A).

For quantitative estimation of overall mitochondrial respiratory function, we isolated immortalized 3T3 cell lines from mouse embryonic fibroblasts (MEFs) by using the 3T3 protocol [18,19]. Immortalized 3T3 cell lines obtained from m/m mutator mice (3T3m/m) and mito-miceΔ (3T3Δ) showed a similar reduction in both COX activity (Fig. 1A) and O_2 consumption rates compared to controls (Fig. 1B). Thus, m/m mutator mice express notable respiration defects, even when they share B6J nuclear genetic background with that of mito-miceΔ.

Cotransfer of mtDNA and Respiration Defects from m/m Mice into ρ^0 Mouse B82 Cells

We then addressed whether respiration defects found in mtDNA mutator mice (Fig. 1) are caused by abnormalities accumulated in mtDNA or in nuclear DNA. It is possible that the genetic complementation activity present in mammalian mitochondria [10,15,16] prevents tissues from expressing respiration defects caused by the accumulated random mutations in mtDNA. Moreover, considering that respiratory functions are controlled by both mtDNA and nuclear DNA, it is still possible that abnormalities in nuclear DNA are responsible for respiration defects, even though mtDNA mutator mice are prone to accumulate various somatic mutations in mtDNA [6,7,21–23].

To examine this possibility, we transferred mitochondria from the platelets of +/m and m/m mutator mice (10 months old) into ρ^0 mouse B82 cells by their fusion with the platelets. Selection medium without uridine and pyruvate excluded the unfused ρ^0 mouse B82 cells, and allowed exclusive growth of B82mt+/m and B82mtm/m transmitochondrial cybrids, which share the B82 nuclear background but carry mtDNA from +/m and m/m mice, respectively (Table S1). As positive controls, we used B82mtWT transmitochondrial cybrids, which were obtained by the fusion of ρ^0 mouse B82 cells with the platelets from age-matched wild-type (WT) B6J mice (Table S1).

All isolated transmitochondrial cybrids were cultivated for 2 months to obtain a sufficient number of cells to estimate O_2 consumption rates. COX activity (Fig. 2A) and O_2 consumption rates (Fig. 2B) were reduced significantly in B82mtm/m cybrids compared to controls. These results suggest that mitochondrial respiration defects were co-transferred with the mtDNA from m/m mice into ρ^0 mouse B82 cells, providing convincing evidence that respiration defects expressed in mtDNA mutator mice are due to mtDNA abnormalities created by the deficient proofreading function of mtDNA polymerase. Moreover, these observations also suggest that the transferred respiration defects were not restored during the prolonged 2-month long cultivation of B82mtm/m cybrids, even under conditions where the nuclear genome of the cybrids was derived from B82 cells possessing mtDNA polymerase with a normal proofreading function. Therefore, mtDNA abnormalities are furthermore transferable to following generations of the cybrids, and would correspond to mtDNA mutations.

Sequence and Southern Blot Analyses of mtDNA from m/m Mice

To examine whether the mtDNA abnormalities correspond to point mutations or deletion mutations of mtDNA, we carried out sequence analysis (Fig. 3A) and Southern blot analysis (Fig. 3B) of mtDNA prepared from the heart of an m/m mouse (10 months old) and B82mtm/m cybrids. The heart of an age-matched B6J (wild-type) mouse and B82mtWT cybrids were used as controls.

Sequence analysis of fifty clones of a part of *COX1* gene revealed that significant amounts of point mutations are accumulated in mtDNA from the heart of an m/m mutator mouse, while no mutations were found in the heart of an age-matched B6J mouse (Fig. 3A). Preferential accumulation of somatic point mutations in mtDNA was also observed in B82mtm/m cybrids, when we compared mtDNA sequence between B82mtm/m and B82mtWT cybrids (Fig. 3A). Therefore, enhanced accumulation of the mtDNA point mutations would partly be responsible for the respiration defects found in tissues of m/m mutator mice (Fig. 1) and in B82mtm/m cybrids (Fig. 2).

Southern blot analysis also showed that the heart of an m/m mouse possessed deleted mtDNA fragments (about 8 kbp) as well as mtDNA with normal sizes (about 16 kbp). However, B82mtm/m cybrids did not possess detectable amounts of the deleted mtDNA fragments (Fig. 3B). These observations suggest that the deleted mtDNA produced in the tissues of the m/m mouse can partly be responsible for the respiration defects (Fig. 1), but are not able to replicate and confer respiration defects in B82mtm/m cybrids (Fig. 2). Thus, the deleted products would correspond to the linear mtDNA fragments newly created by the mutated polymerase gamma of m/m mice [22], but not to mtDNA with deletion mutations.

Lifespan and Premature Aging Phenotypes

Next, we investigated whether homozygous m/m mutator mice carrying a B6J nuclear background also express premature aging phenotypes. To examine this idea we started the experiments using 6-month-old mice: 19 wild-type B6J mice, 71 mtDNA mutator mice (39+/m and 32 m/m), and 25 mito-mice$\Delta^{2.0–60.8}$ with 2.0–60.8% ΔmtDNA in their tails at 4 weeks after the birth.

Median survival times of wild-type, +/m, and m/m mutator mice were 26, 27, and 10 months, respectively (Fig. 4A), showing that homozygous m/m mutator mice have a much shorter lifespan than controls, even under a B6J nuclear background. Median survival times of 10 months for our m/m mutator mice with a B6J nuclear background is slightly shorter than the 11 months [6] and 14 months [7] of other m/m mutator mice (Table S2), probably due to the differences in nuclear background and/or conditions for feeding and maintenance.

When the proportions of ΔmtDNA in tails were restricted to higher levels (40.0%–60.8%), 13 mito-mice$\Delta^{40.0–60.8}$ possessing 40.0%–60.8% ΔmtDNA in their tails had a very short lifespan (9 months; Fig. 4A) comparable to that of m/m mutator mice (10 months; Fig. 4A). Thus, damages of mtDNA would be very similar between m/m mice and mito-mice$\Delta^{40.0–60.8}$. Moreover, all 13 mito-mice$\Delta^{40.0–60.8}$ showed kyphosis (Fig. 4B), which has been observed in m/m mutator mice [6,7] and confirmed in this study to be expressed in m/m mutator mice with a B6J nuclear background (Figs. 4B and Table S2). However, alopecia, which has been reported in m/m mutator mice as a typical premature aging phenotype [6,7], was not observed in our m/m mutator mice and mito-mice$\Delta^{40.0–60.8}$ sharing the same B6J nuclear background (Fig. 4B). The absence of alopecia in both our m/m mutator mice and mito-mce$\Delta^{40.0–60.8}$ suggest that the apparent discrepancy in the expression of premature aging phenotypes that were observed exclusively in mtDNA mutator mice [6,7], but not in mito-miceΔ [9,10] might partly be related to slight differences in their nuclear genetic background (Table S2).

Moreover, both the homozygous m/m mutator mice with a B6J nuclear background and mito-mce$\Delta^{40.0–60.8}$ had low blood glucose

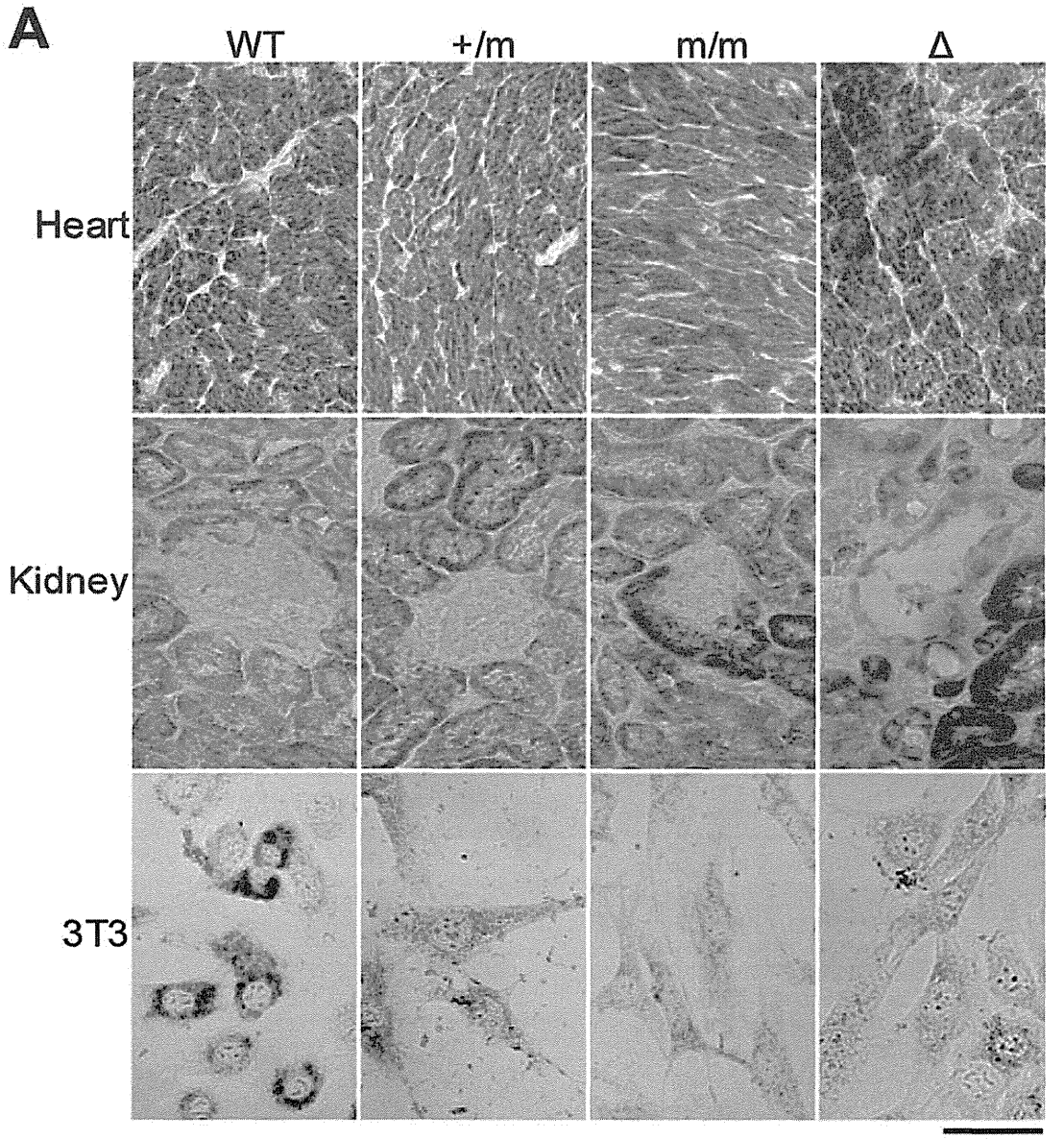
A
WT
+/m
m/m
Δ
Heart
Kidney
3T3
B
O2 consumption rates (%)
100
50
0
3T3WT
3T3+/m
3T3m/m
3T3Δ
*
*

Figure 1. Comparison of mitochondrial respiratory function in mtDNA mutator mice and mito-miceΔ. WT, wild-type mice; +/m, heterozygous mutator mice; m/m, homozygous mutator mice; Δ, mito-miceΔ. (A) Histochemical analysis of mitochondrial respiratory enzyme activities in the heart, kidney, and 3T3 cells. Tissue sections and 3T3 cells were stained for cytochrome *c* oxidase (COX) (brown) and succinate dehydrogenase (SDH) (blue). Cells that had lost COX activity were detected as a blue colour. The proportions of ΔmtDNA in the heart, kidney tissues, and 3T3 cells from mito-miceΔ were 82.6%, 79.1%, and 73.8%, respectively. A scale bar, 50 μm. (B) Measurement of O_2 consumption rates in 3T3 cells. Data are represented as mean values with SD (n = 3). *P<0.05 compared with wild-type mice.
doi:10.1371/journal.pone.0055789.g001

and high blood lactate levels, while heterozygous +/m mutator mice were normal in their levels (Fig.4C). These results are consistent with the findings of previous studies [9,24,25] with the exception that m/m mutator mice with a B6J nuclear background have low blood glucose levels (Fig. 4C). These observations suggest that homozygous m/m mutator mice have potential as a model for the study of mitochondrial diseases as well as of aging. However, our m/m mutator mice and mito-mce$\Delta^{40.0-60.8}$ sharing the B6J nuclear background also showed different phenotypes associated with diseases. For example, m/m mutator mice expressed significant increase in the amounts of blood lactate levels (Fig. 4C). On the contrary, mito-miceΔ exclusively had enlarged kidneys with a granulated surface with renal failures [10]. Considering that mito-miceΔ accumulated the same ΔmtDNA with age, and that m/m mutator mice accumulated mtDNA with various somatic mutations with age, the difference of mutations in mtDNA may partly be responsible for the difference of their phenotypes.

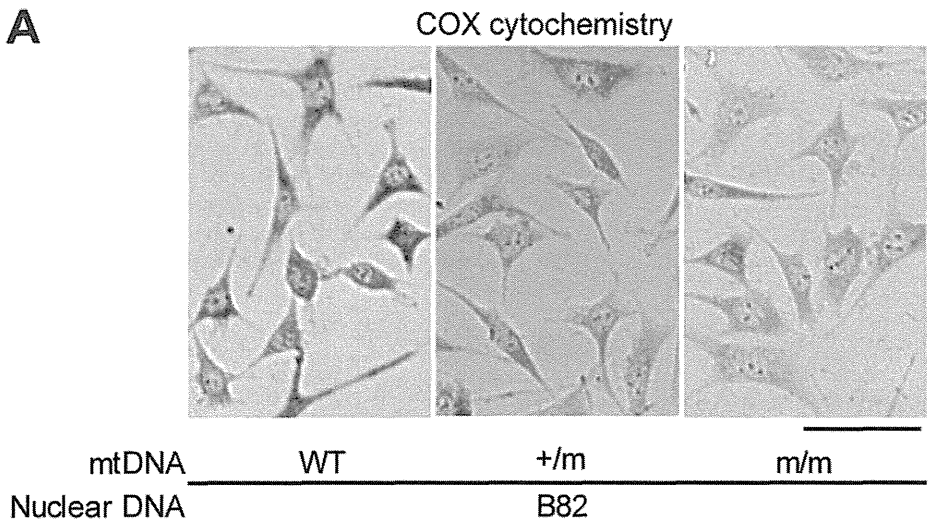

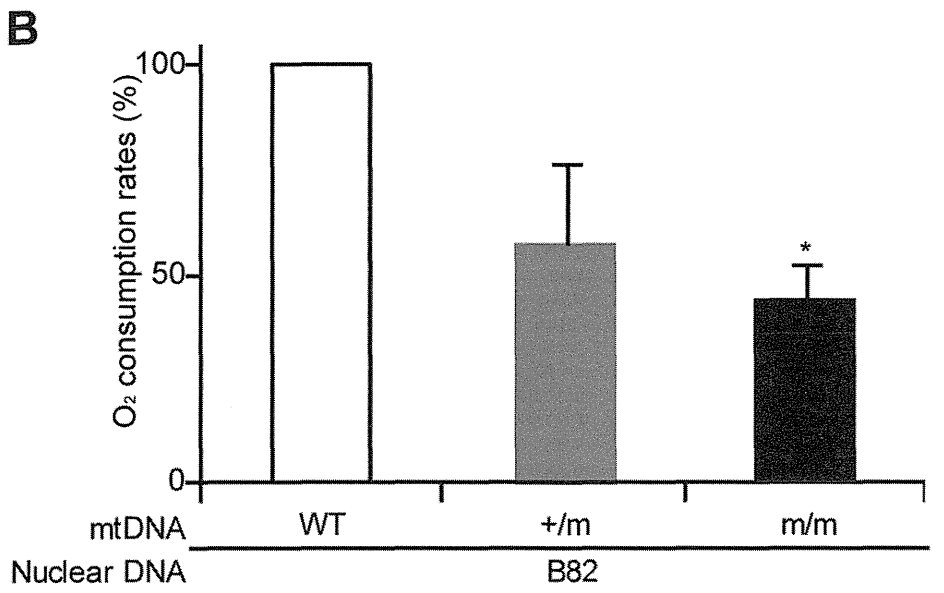

Figure 2. Cotransfer of mtDNA and respiration defects from mtDNA mutator mice into ρ^0 mouse B82 cells. WT, wild-type mice; +/m, heterozygous mutator mice; m/m, homozygous mutator mice. (A) Cytochemical analysis of mitochondrial respiratory enzyme activities in trans-mitochondrial cybrids. Cells that had lost COX activity were detected as a blue colour. A scale bar, 50 μm. (B) Measurement of O_2 consumption rates. Data are represented as mean values with SD (n = 3). *P<0.05 compared with wild-type mice.
doi:10.1371/journal.pone.0055789.g002

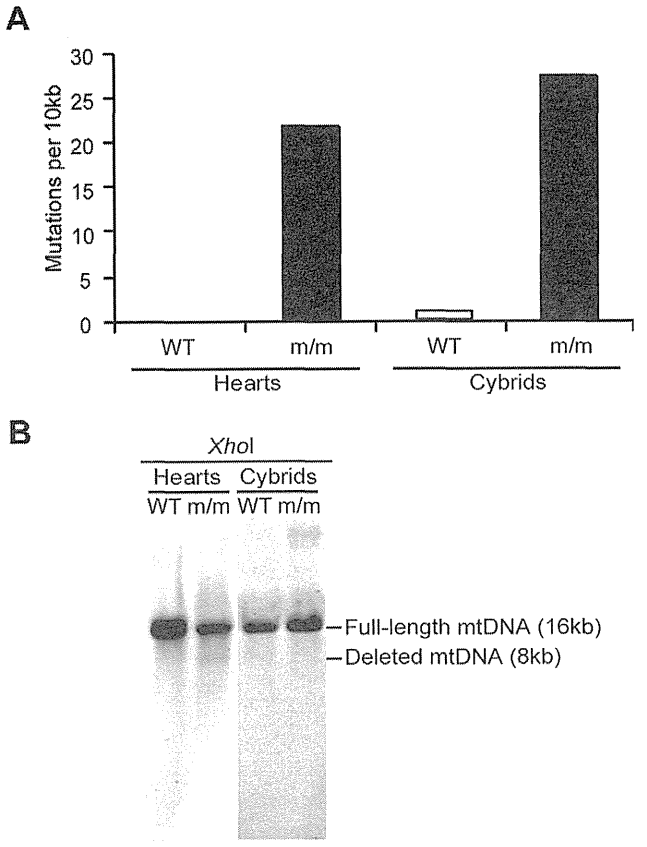

Figure 3. Sequence and Southern blot analyses of mtDNA from mtDNA mutator mice. Total DNA was prepared from the hearts of a 10-month-old wild-type mouse (WT) and an age matched homozygous mutator mouse (m/m), and from the trans-mitochondrial cybrids carrying mtDNA from platelets of a 10-month-old wild-type mouse and age-matched m/m mutator mouse, respectively. (A) Sequence analysis of 517 bp-fragments of the *COX1* gene. Numbers of somatic mutations in mtDNA of the hearts from a wild-type mouse and an m/m mouse, and of the cybrids with mtDNA of a wild-type and an m/m mouse were counted. (B) Southern blot analysis of *Xho*I-digested mtDNA. Lanes 1 and 2 represent the hearts of a WT and an m/m mouse, respectively. Lanes 3 and 4 represent the cybrids with mtDNA of a wild-type and an m/m mouse, respectively.
doi:10.1371/journal.pone.0055789.g003

Tumor Formation Frequencies of +/m Mice

Although heterozygous +/m mutator mice showed mild respiration defects (Fig. 1), they had a normal lifespan (Fig. 4A) that was comparable to a lifespan of wild-type mice. These results are consistent with the findings of a previous study [26] that showed that median survival times of +/m mice did not change substantially from those of wild-type mice. However, gross necropsy of all dead or euthanized moribund mice revealed that 15 of 29+/m mutator mice (52%) had macroscopic tumor-like abnormalities in spleen, liver and/or lymph nodes (Table S3 and Fig. 5A). By comparison, only 2 of 12 wild-type mice (17%) and none of the 32 m/m mutator mice showed tumor-like abnormalities (Table S3).

Histological analyses revealed that all abnormal tissues were hematopoietic neoplasms and were positive for the pan-leukocyte marker CD45 (Table S3 and Fig. 5B). Since there was no increase in the number of leukemic cells in the peripheral blood of +/m mice compared with wild-type mice (Fig. 5A), these hematological neoplasms most likely consisted of lymphoma cells. All tumors were of B-cell origin because they expressed the B-cell marker B220 (Fig. 5B), and arose in the spleen, liver, lung, and/or lymph nodes (Table S3 and Fig. 5A). These data indicated that compared to wild-type mice, the +/m mutator mice were more prone to B-cell lymphoma development.

The median survival times of +/m mutator mice with and without B-cell lymphoma were 26 and 28 months, respectively (Fig. 5C). The shorter lifespan of +/m mutator mice with B-cell lymphoma compared with that of +/m mutator mice without B-cell lymphoma is most likely partly the result of B-cell lymphoma development.

Estimation of ROS in Bone Marrows of +/m Mice with and without B-cell Lymphomas

Our previous report showed that aged mito-miceND6^{M} carrying an mtDNA point mutation G13997A in the *ND6* gene frequently developed B cell-lymphomas [14]. Because bone marrow cells of mito-miceND6^{M} overproduce ROS [14], the overproduction of ROS in bone marrow cells of +/m mutator mice might be crucial for the development of B-cell lymphoma (Table S3). To examine this idea, we compared the amount of mitochondrial ROS in the bone marrow cells of wild-type mice with that of +/m mutator mice (20–25 months old). An increase in the amount of mitochondrial ROS was observed only in +/m mutator mice with B-cell lymphomas (Fig. 6). It is therefore likely that the overproduction of ROS in bone marrow cells of +/m mutator mice plays an important part in the formation of B-cell lymphoma.

Discussion

By generating mtDNA mutator mice with the same B6J nuclear background as that of mito-miceΔ, we can provide an answer to the question of why premature aging phenotypes are exclusively observed in homozygous m/m mutator mice but not in transmitochondrial mito- miceΔ, even though they both express significant respiration defects. We showed that the significant respiration defects and high frequency of mtDNA mutations were expressed in m/m mutator mice generated here, and can be transferred together with the transfer of mtDNA from the platelets of the m/m mutator mice into ρ^0 B82 cells (Figs. 1, 2, 3). Thus, our mutator mice also express respiration defects, even under a B6J nuclear background, and respiration defects found in mutator mice are caused by abnormalities in their mtDNA. However, the m/m mutator mice with a B6J nuclear background did not express the premature aging phenotypes of graying and alopecia, while they did express kyphosis and had a short lifespan (Fig. 4). Similar phenotypes were observed in mito-mice$\Delta^{40.0-60.8}$, when the proportions of ΔmtDNA were restricted to higher levels (Fig. 4). Therefore, the expression patterns of premature aging phenotypes of m/m mutator mice with a B6J nuclear background are very similar to that of mito-miceΔ carrying predominant amounts of ΔmtDNA in that they both express kyphosis and have a short lifespan, but do not express graying and alopecia. These observations suggest that the apparent discrepancy in the presence and absence of premature aging phenotypes in mutator mice and mito-mice from previous studies is partly the result of differences in their nuclear genetic background.

Heterozygous +/m mutator mice showed only slight respiration defects (Figs. 1 and 2) and had a normal lifespan comparable to that of wild-type mice (Fig. 4A), which are findings consistent with a previous publication [26]. However, this study provided the new evidence that +/m mutator mice with a B6J nuclear background frequently develop age-associated B-cell lymphomas. The +/m

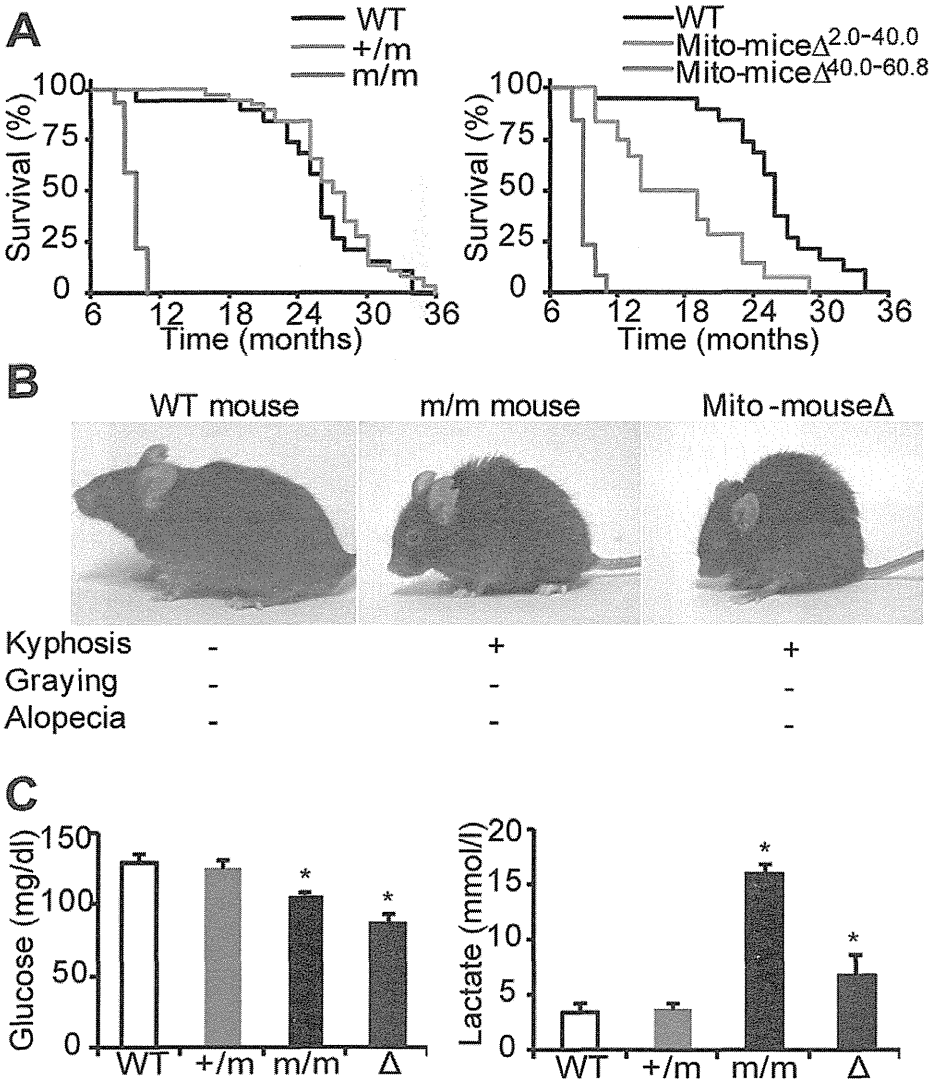

Figure 4. Comparison of the phenotypes observed in mtDNA mutator mice and mito-miceΔ. (A) Kaplan–Meier survival curves of mtDNA mutator mice and mito-miceΔ. Median survival times of wild-type (WT) mice (n = 19), +/m mice (n = 39), m/m mice (n = 32), mito-miceΔ$^{2.0-40.0}$ (n = 12), and mito-miceΔ$^{40.0-60.8}$ (n = 13) were 26, 27, 10, 17, and 9 months, respectively. (B) WT mouse, m/m mouse, and mito-mouseΔ at 9 months of age. Kyphosis was observed in homozygous m/m mutator mice and mito-miceΔ, while hair graying and hair loss (alopecia) were not observed. (C) Estimation of blood glucose and blood lactate levels in mutator mice and mito-miceΔ$^{40-60.8}$ at 9 months of age. WT, wild-type mice; +/m, heterozygous mutator mice; m/m, homozygous mutator mice; Δ, mito-miceΔ. Data are represented as mean values with SD (n = 3). *$P<0.05$ compared with wild-type mice.
doi:10.1371/journal.pone.0055789.g004

mutator mice developed no tumors other than B-cell lymphomas (Table S3), despite the presence of mtDNA abnormalities in all the tissues. Considering that 17% of the wild-type mice formed B-cell lymphoma but no other tumors (Table S3), one answer to this tissue-specific tumor development in +/m mice is that the nuclear background of the B6J mice used in this study made them prone to the development of B-cell lymphomas. In support of this notion, it has been reported that the nuclear genetic background affects the spectrum of tumors that develop in mice [27–30].

With respect to the mechanism underlying the development of B-cell lymphoma in +/m mice, the overproduction of ROS in bone marrow cells may be related, because oxidative stress induces various types of cellular damages that can lead to genetic instability and subsequent tumor development [31]. However, it has been reported that tissues and cells from mtDNA mutator mice do not overproduce ROS [7,8,32]. Our study also showed that bone marrow cells in +/m mice do not overproduce mitochondrial ROS (Fig. 6). In contrast, bone marrow cells from +/m mice carrying B-cell lymphomas exclusively overproduced mitochondrial ROS (Fig. 6). It is therefore possible that a population of bone marrow cells was induced to overproduce ROS as the results of B-cell lymphoma development. It is also possible that a small population of bone marrow cells accumulates specific mtDNA abnormalities that, by chance, induce ROS overproduction resulting in the development of B-cell lymphoma. The latter idea is supported by our recent findings that B-cell lymphomas developed preferentially in transmitochondrial mito-miceND6^{M} carrying a ROS-inducing mtDNA mutation [14] but not in transmitochondrial mito-miceCOI^{M} carrying an mtDNA point mutation that does not induce ROS overproduction [14]. Taken together, these observations suggest that mtDNA abnor-

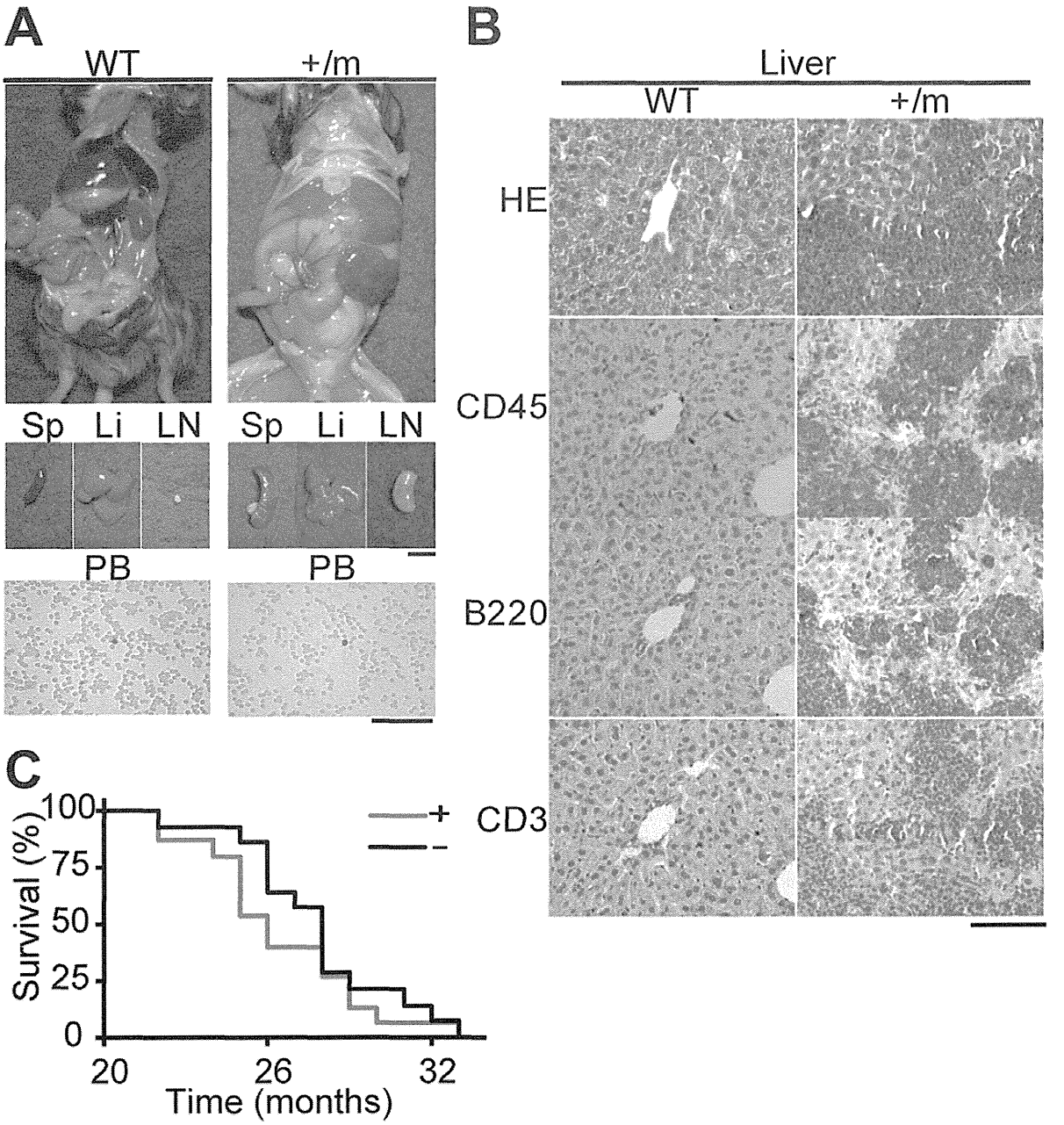

Figure 5. B-cell lymphoma formation in the tissues of aged +/m mutator mice. WT, wild-type mice; +/m, heterozygous mutator mice. (A) Gross necropsy of euthanized moribund mice (upper panels), tissues (middle panels), and smear samples of peripheral blood stained with Giemsa (lower panels). Left and right panels represent a euthanized moribund wild-type (WT) mouse without tumors and a euthanized moribund +/m mouse with tumors (+/m mouse-4; see Table S2), respectively. Giemsa-stained preparations show the absence of leukemic cells in the peripheral blood of both wild-type and +/m mice. Sp, spleen; Li, liver; LN, lymph node; PB, peripheral blood. Scale bars represent 1 cm (middle panels) and 50 μm (lower panels). (B) Histological analyses of serial sections of the liver to identify B-cell lymphoma. Hematoxylin and eosin (HE) staining to show tumor formation; CD45, immunohistochemistry using antibody to CD45 to detect leukocytes; B220, immunohistochemistry using antibody to B220 to detect B cells; CD3, immunohistochemistry using antibody to CD3 to detect T cells. The tissues of WT mice have a normal structure (left), whereas those of +/m mice show of the development of B-cell lymphoma, because they stained positively with CD45 and B220, but not with CD3 (right). A scale bar, 50 μm. (C) Kaplan–Meier survival curves of +/m mice with or without lymphoma. Median survival times of +/m mice with lymphoma (n = 15) and +/m mice without lymphoma (n = 14) were 26 and 28 months, respectively. +, +/m mice with lymphoma; −, +/m mice without lymphoma; $P = 0.362$.

doi:10.1371/journal.pone.0055789.g005

malities in +/m mice do not accelerate aging (Fig. 4A), but preferentially induce B-cell lymphoma development (Table S3).

Because our previous studies [10,15,16] demonstrated the presence of inter-mitochondrial interactions and the resultant genetic complementation that occurs in mammalian mitochondria, it is possible that accumulated random mutations in mtDNA complemented each other and fail to induce the respiration defects found in mtDNA mutator mice. However, this study provided convincing evidence that respiration defects can be transferred together with mtDNA from mtDNA mutator mice into ρ^0 mouse

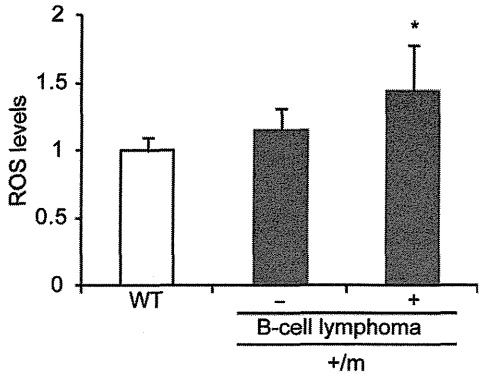

Figure 6. Estimation of mitochondrial ROS levels in bone marrow cells of +/m mice with and without B-cell lymphoma. WT, wild-type mice; +/m, heterozygous mutator mice; −, mice without lymphoma; +, mice with lymphoma. Relative mitochondrial superoxide levels in +/m mice without B-cell lymphoma and +/m mice with B-cell lymphoma were expressed as mean uorescence intensity after treatment with MitoSOX Red (Life Technologies). Data are represented as mean values with SD (n = 5). *$P<0.05$ compared with wild-type mice.
doi:10.1371/journal.pone.0055789.g006

B82 cells (Fig. 2). These findings suggest that respiration defects in mtDNA mutator mice (Fig. 1) are caused by abnormalities in their mtDNA. One explanation of why random mutations in the mtDNA of mtDNA mutator mice induce respiration defects in the presence of mitochondrial genetic complementation is that the extremely high frequency of somatic mutations in mtDNA causes instability of the large mitochondrial respiration complexes thereby resulting in respiration defects, even when somatic mutations occur at random sites [23]. This idea could be examined by complete sequence analysis of mtDNA in tissues of m/m mice.

Supporting Information

Table S1 Isolation of the trans-mitochondrial cybrids. [a]B82 cells are fibrosarcomas derived from the L929 fibroblast cell line (C3H/An mouse strain), and ρ^0 B82 cells without their own mtDNA were isolated in our previous report (9). [b]UP- represent the selection medium without uridine and pyruvate to exclude unfused ρ^0 B82 cells.
(DOC)

Table S2 Characterization of the mice used in the previous studies and this study. [a] A B6J strain used in this study corresponds to a B6JJcl strain generated by sibling mating more than 40 times in CLEA Japan (Jcl). [b] Expression of a hair graying phenotype is not detectable in this strain because of its phenotypic expression of white hair color [6]. [c] Alopecia was observed in m/m mice with B6 strain nuclear genome [7] and in m/m mice with 129R1/B6 strain nuclear genome [6], but not in m/m mice with B6JJcl nuclear genome generated in this study. Since nuclear genomes are very close between B6 strain used in the previous study [7] and B6JJcl strain used in this study, variability of nuclear genome may not be responsible for the lack of alopecia in our m/m mice. On the contrary, this study also showed that m/m mice as well as mito-miceΔ sharing the same B6JJcl nuclear genetic background and feeding conditions did not express alopecia (Fig. 4), suggesting that slight variability of nuclear genome between B6 and B6JJcl mice and/or different conditions for feeding and maintenance may due at least in part to the discrepancy that the alopecia was not observed in m/m mice of this study.
(DOC)

Table S3 Frequencies of lymphoma in dead or moribund mice. [a] Individual codes were allocated in order of death.
(DOC)

Author Contributions

Conceived and designed the experiments: TM JIH. Performed the experiments: TM Y. Kikkawa AS OH SK HI AO Y. Kato. Analyzed the data: TM Y. Kikkawa AS OH SK HI AO KN JIH. Wrote the paper: JIH.

References

1. Wallace DC (1999) Mitochondrial diseases in man and mouse. Science 283: 1482–1488.
2. Taylor RW, Turnbull DM (2005) Mitochondrial DNA mutations in human disease. Nat Rev Genet 6: 389–402.
3. Jacobs HT (2003) The mitochondrial theory of aging: dead or alive? Aging Cell 2: 11–17.
4. Khrapko K, Vija J (2008) Mitochondrial DNA mutations and aging: devils in the details? Trends Genet 25: 91–98.
5. Loeb LA, Wallace DC, Martin GM (2005) The mitochondrial theory of aging and its relationship to reactive oxygen species damage and somatic mtDNA mutations. Proc Natl Acad Sci U S A 102: 18769–18770.
6. Trifunovic A, Wredenberg A, Falkenberg M, Spelbrink JN, Rovio AT, et al. (2004) Premature ageing in mice expressing defective mitochondrial DNA polymerase. Nature 429: 417–423.
7. Kujoth GC, Hiona A, Pugh TD, Someya S, Panzer K, et al. (2005) Mitochondrial DNA mutations, oxidative stress, and apoptosis in mammalian aging. Science 309: 481–484.
8. Trifunovic A, Hansson A, Wredenberg A, Rovio AT, Dufour E, et al. (2005) Somatic mtDNA mutations cause aging phenotypes without affecting reactive oxygen species production. Proc Natl Acad Sci U S A 102: 17993–17998.
9. Inoue K, Nakada K, Ogura A, Isobe K, Goto Y-I, et al. (2000) Generation of mice with mitochondrial dysfunction by introducing mouse mtDNA carrying a deletion into zygotes. Nat Genet 26: 176–181.
10. Nakada K, Inoue K, Ono T, Isobe K, Ogura A, et al. (2001) Inter-mitochondrial complementation: Mitochondria-specific system preventing mice from expression of disease phenotypes by mutant mtDNA. Nat Med 7: 934–940.
11. Kasahara A, Ishikawa K, Yamaoka M, Ito M, Watanabe N, et al. (2006) Generation of trans-mitochondrial mice carrying homoplasmic mtDNAs with a missense mutation in a structural gene using ES cells. Hum Mol Genet 15: 871–881.
12. Yokota M, Shitara H, Hashizume O, Ishikawa K, Nakada K, et al. (2010) Generation of trans-mitochondrial mito-mice by the introduction of a pathogenic G13997A mtDNA from highly metastatic lung carcinoma cells. FEBS Lett 584: 3943–3948.
13. Ishikawa K, Takenaga K, Akimoto M, Koshikawa N, Yamaguchi A, et al. (2008) ROS-generating mitochondrial DNA mutations can regulate tumor cell metastasis. Science 320: 661–664.
14. Hashizume O, Shimizu A, Yokota M, Sugiyama A, Nakada K, et al. (2012) Specific mitochondrial DNA mutation in mice regulates diabetes and lymphoma development. Proc Natl Acad Sci U S A 109: 10528–10533.
15. Hayashi J-I, Takemitsu M, Goto Y-i, Nonaka I (1994) Human mitochondria and mitochondrial genome function as a single dynamic cellular unit. J Cell Biol 125: 43–50.
16. Ono T, Isobe K, Nakada K, Hayashi J-I (2001) Human cells are protected from mitochondrial dysfunction by complementation of DNA products in fused mitochondria. Nat Genet 28: 272–275.
17. Littlefield JW (1964) Selection of hybrids from matings of fibroblasts in vitro and their presumed recombinants. Science 145: 709–710.
18. Todaro GJ, Green H (1963) Quantitative studies of the growth of mouse embryo cells in culture and their development into established lines. J Cell Biol 17: 299–313.
19. Sun H, Taneja R (2007) Analysis of transformation and tumorigenicity using mouse embryonic fibroblast cells. Methods Mol Biol 383: 303–310.
20. Sato A, Kono T, Nakada K, Ishikawa K, Inoue S, et al. (2005) Gene therapy for progeny of mito-mice carrying pathogenic mtDNA by nuclear transplantation. Proc Natl Acad Sci U S A 102: 16765–16770.

21. Vermulst M, Wanagat J, Kujoth GC, Bielas JH, Rabinovitch PS, et al. (2008) DNA deletions and clonal mutations drive premature aging in mitochondrial mutator mice. Nat Genet 40: 392–394.
22. Bailey LJ, Cluett TJ, Reyes A, Prolla TA, Poulton J, et al. (2009) Mice expressing an error-prone DNA polymerase in mitochondria display elevated replication pausing and chromosomal breakage at fragile sites of mitochondrial DNA. Nucleic Acids Res 37: 2327–2335.
23. Edgar D, Shabalina I, Camara Y, Wredenberg A, Calvaruso MA, et al. (2009) Random point mutations with major effects on protein-coding genes are the driving force behind premature aging in mtDNA mutator mice. Cell Metab 10: 131–138.
24. Ross JM, Öberg J, Brené S, Coppotelli G, Terzioglu M, et al. (2010) High brain lactate is a hallmark of aging and caused by a shift in the lactate dehydrogenase A/B ratio. Proc Natl Acad Sci U S A 107: 20087–20092.
25. Nakada K, Sato A, Sone H, Kasahara A, Ikeda K, et al. (2004) Accumulation of pathogenic ΔmtDNA induced deafness but not diabetic phenotypes in mito-mice. Biochem Biophys Res Commun 323: 175–184.
26. Vermulst M, Bielas JH, Kujoth GC, Ladiges WC, Rabinovitch PS, et al. (2007) Mitochondrial point mutations do not limit the natural lifespan of mice. Nat Genet 39: 540–543.
27. Krupke DM, Begley DA, Sundberg JP, Bult CJ, Eppig JT (2008) The Mouse Tumor Biology database. Nat Rev Cancer 8: 459–465.
28. Balmain A, Nagase H (1998) Cancer resistance genes in mice: models for the study of tumour modifiers. Trends Genet 14: 139–144.
29. Harvey M, McArthur MJ, Montgomery Jr CA, Bradley A, Donehower LA (1993) Genetic background alters the spectrum of tumors that develop in p53-deficient mice. FASEB J 7: 938–943.
30. Freeman D, Lesche R, Kertesz N, Wang S, Li G, et al. (2006) Genetic background controls tumor development in PTEN-deficient mice. Cancer Res 66: 6492–6496.
31. Klaunig JE, Kamendulis LM, Hocevar BA (2010) Oxidative stress and oxidative damage in carcinogenesis. Toxicologic Pathol 38: 96–109.
32. Norddahl GL, Pronk CJ, Wahlestedt M, Sten G, Nygren JM, et al. (2011) Accumulating mitochondrial DNA mutations drive premature hematopoietic aging phenotypes distinct from physiological stem cell aging. Cell Stem Cell 6: 499–510.

27巻2号 148～154頁（2013年）

●原　　著●

ミトコンドリア呼吸鎖複合体異常症における消化器症状についての検討

（平成25年2月4日受付，平成25年4月8日受理）

*1千葉県こども病院代謝科
*2同　新生児科
*3埼玉医科大学小児科
*4現　佐賀大学医学部附属病院小児科

川内　恵美*1*4・村山　圭*1・伏見　拓矢*1・市本　景子*2
鶴岡　智子*2・高柳　正樹*1・大竹　明*3

Key Words：ミトコンドリア呼吸鎖異常症，難治性下痢症，胆汁性嘔吐，胃食道逆流，pseudo-obstruction

要　旨

ミトコンドリア呼吸鎖複合体異常症（MRCD）は多彩な症状を呈する，最も頻度の高い先天代謝異常症であり，消化器症状も例外ではない。我々の施設でMRCDと診断した189例のうち，消化器症状を認めた症例は56例あり，このうち消化器症状が主症状であった症例は25例で，難治性下痢症，嘔吐症，胃食道逆流症，壊死性腸炎の順に多く認められた。消化器症状の多くが1歳以内に発症し，新生児期発症が過半数を占めていた。診断に至った検体は肝臓，次いで筋肉であり，酵素活性低下により診断した。残り31例の消化器症状は呼吸障害や心不全，乳酸アシドーシスやけいれんなどに伴う随伴症状と考えられた。生後早期の哺乳不良や消化器症状が持続する場合，経時的な他臓器の評価や高乳酸血症の評価など，MRCDも念頭に置いた精査が必要である。

はじめに

ミトコンドリア呼吸鎖複合体異常症（MRCD）は，生体内のエネルギー源となるATP産生にもっとも関わる呼吸鎖（電子伝達系）の障害，もしくはその反応である酸化的リン酸化の障害により引き起こされる1/5000の発症頻度の疾患である。罹患臓器も多臓器にまたがり，臨床症状も多彩である[1]。MRCDにおける消化器症状は，体全体のATP使用量の20%を占める脳や肝臓，重量あたりのATP使用量が高い心臓，腎臓といった高エネルギー臓器の機能障害とは異なり，それが唯一の特徴的症状であることは稀であるが，認められる頻度は高く，症状の一部として見落とされやすいとされる[2]。我々がこれまでに診断したMRCD症例において，消化器症状を呈した症例について検討したので報告する。

別刷請求先：〒849-8501　佐賀県佐賀市鍋島5丁目1－1
佐賀大学医学部附属病院小児科
川内　恵美

対象と方法

2007年より2012年までに，臨床症状や高乳酸血症，高アラニン血症の存在，画像所見などから，ミトコンドリア呼吸鎖異常症が疑われた症例に対し，呼吸鎖の酵素活性およびBlue-nativePAGEを用いたイムノブロット解析を行った。Bernier[3]らの提唱している診断基準を用いて，Definite（確定例）又はProbable（疑い例）と判定した症例を対象とした。いずれも倫理委員会によって承認された承諾書に基づき，十分なインフォームド・コンセントを得て行った。

試料は，－80℃に凍結保存された肝，筋肉，心筋組織と培養皮膚線維芽細胞を用いた。解析方法は，既報[1]のごとくIn vitro酵素活性測定およびBlue-

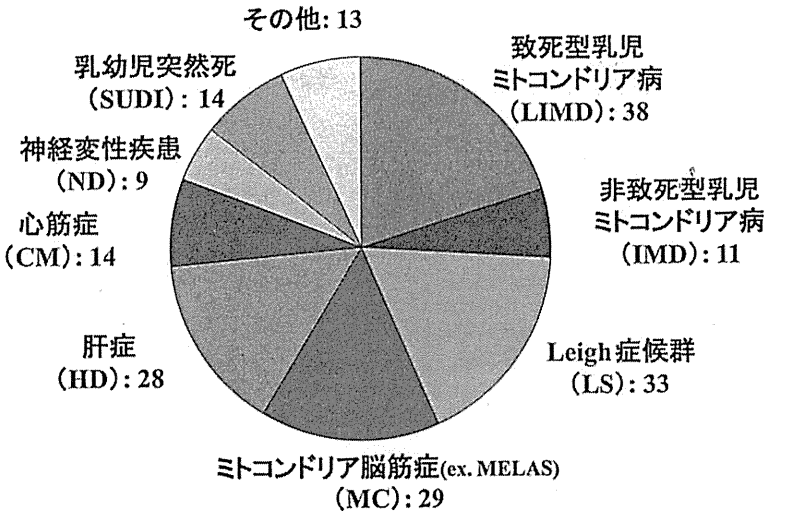

図1　MRCD189例の臨床診断

LIMD：lethal infantile mitochondrial disorder,
IMD：non-lethal infantile mitochondrial disorder,
LS：Leigh'syndrome,
MC：mitochondrial cytopathy,
ND：neurodegenerative disease,
HD：hepatic disease,
CM：cardiomyopathy,
SUDI：sudden unexpected death in infancy

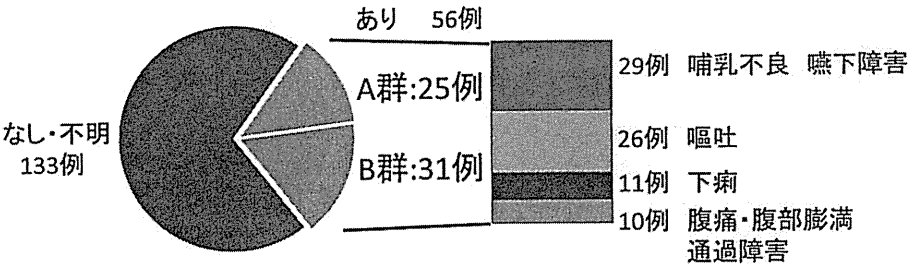

A群：消化器症状が主症状であった症例
B群：消化器症状が新生児仮死，呼吸障害，心不全，
乳酸アシドーシス，けいれんなどの随伴症状であった症例

図2　MRCD189例の消化器症状の内訳

nativePAGEを用いたイムノブロット解析を組み合わせて行った。

消化器症状は，Di Mauro[2]らの文献に基づき哺乳不良・嚥下障害，嘔吐，下痢，腹痛・腹部膨満・通過障害を認めたものとし，診療録や診療情報提供書に初発症状や主訴として記載された症例を対象とした。

結　　果

①MRCD全体について

当施設にて解析を行い，Bernierらの診断基準を用いてDefinite（確定例），Probable（疑い例）と診断した症例は189例であった。男児100例，女児82例，性別不明7例，このうち死亡症例は94例（50%）であった。ミトコンドリア呼吸鎖異常症の特徴の一つとされる高乳酸血症を認めなかった症例が22例（12%）に認められた。

189例の臨床診断を図1に示す。我々の過去の報告[1]と同様，新生児期に難治性の高乳酸血症により発症する乳児ミトコンドリア病が最も多く，致死型38例と非致死型11例で全体の約4分の1を占めていた。

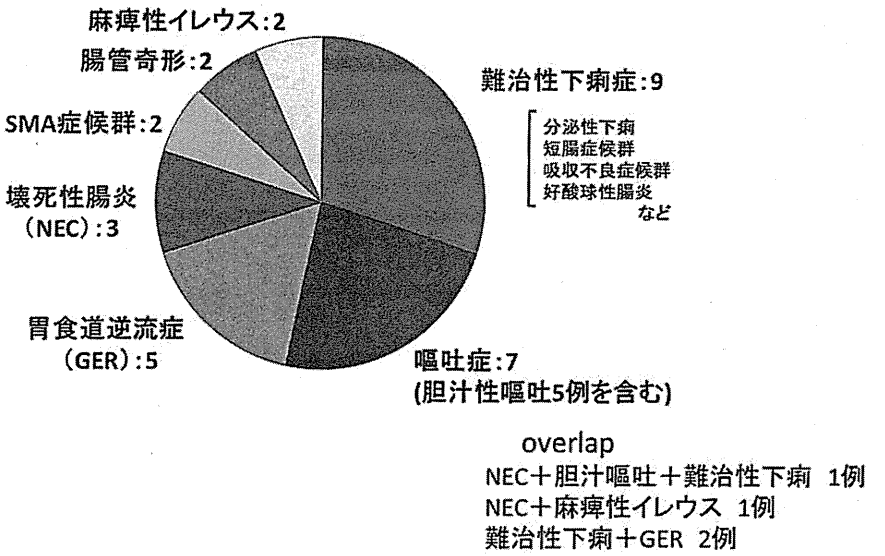

図3　消化器症状が主であったA群25例の内訳

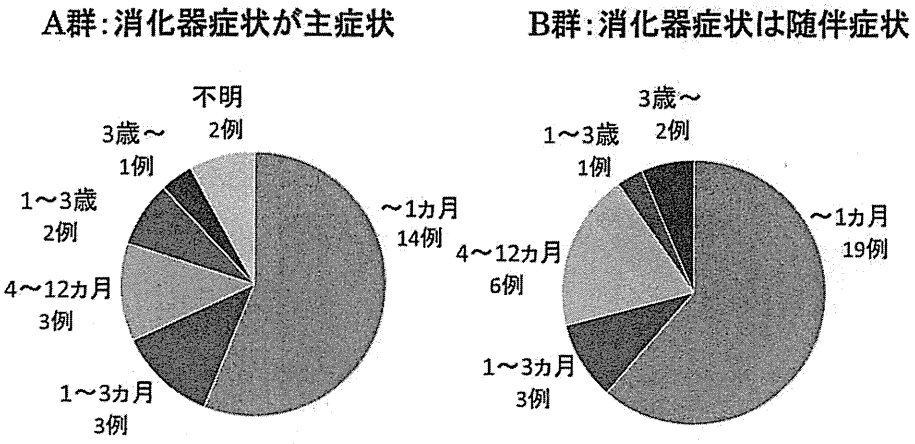

図4　A, B両群における消化器症状の出現時期

次いでLeigh症候群33例，ミトコンドリア脳筋症29例，ミトコンドリア肝症28例，ミトコンドリア心筋症14例となっている。また，乳幼児突然死（sudden unexpected death in infancy:SUDI）に対する原因検索が積極的になされるようになり，MRCDの診断に至った症例が増えており[5]，新たな分類とした。

189例の全体の酵素診断は，Complex I欠損症が86例と最多で，次いで複数の呼吸鎖複合体欠損が68例，Complex Ⅳ欠損症23例，Complex Ⅲ欠損症が9例であった。

②消化器症状を呈したMRCD症例について

1．症状について

MRCD189例における消化器症状の内訳を図2に示す。189例中，消化器症状を呈した症例は56例（30%）であり，哺乳不良・嚥下障害が最も多く，次いで嘔吐，下痢の順に認められ，症状の重複も多かった。このうち臓器症状として消化器症状が主であった症例（A群）は25例で，全体の13%であった。残りの31例（B群）は，新生児仮死や呼吸障害，心不全，乳酸アシドーシス，けいれんなどによる随伴症状であると考えられた。

消化器症状が主であったA群25例の内訳を図3に

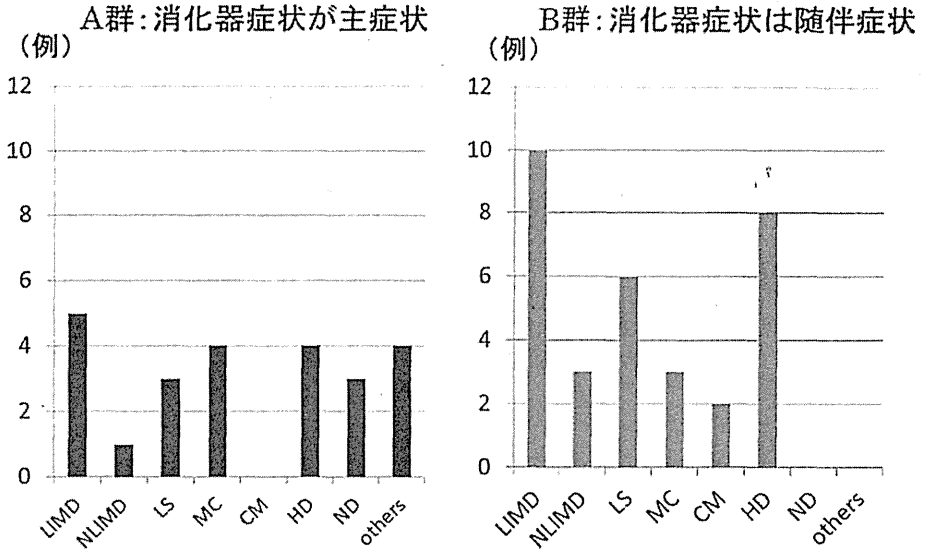

図5　A, B 両群における臨床診断

LIMD：lethal infantile mitochondrial disorder,
NLIMD：non-lethal infantile mitochondrial disorder,
LS：Leigh'syndrome,
MC：mitochondrial cytopathy,
CM：cardiomyopathy,
HD：hepatic disease,
ND：neurodegenerative disease

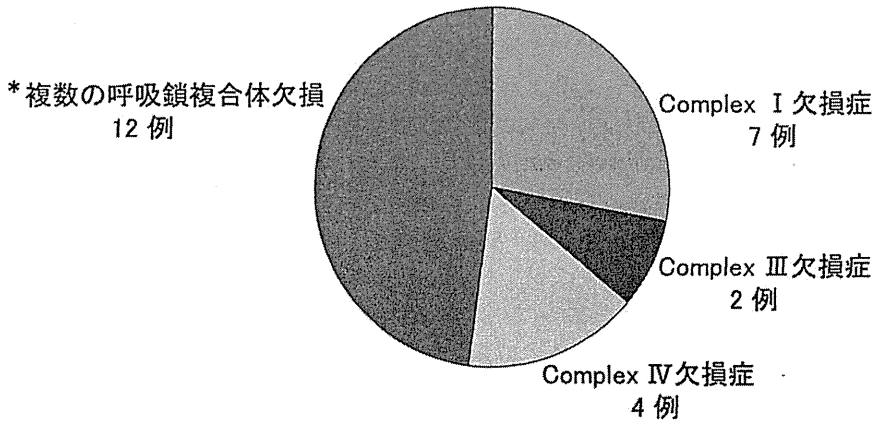

* mtDNA枯渇症候群を2例含む

図6　A 群 25 例の酵素診断

示す。難治性下痢症 9 例，嘔吐症 7 例，胃食道逆流症 5 例，壊死性腸炎 3 例となっており，これらの重複例も認められた。嘔吐症 7 例のうち 5 例に胆汁性嘔吐を認めていた。消化器症状を主徴とする核遺伝子異常の MRCD として知られている Mitochondrial neurogastrointestinal encephalopathy（MNGIE）と臨床診断された症例はなかった。

2．発症時期

A 群と B 群における消化器症状の出現時期を図 4 に示す。A 群では 25 例中，生後 1 ヵ月までに症状が出現した症例が 14 例，1〜3 ヵ月が 3 例，4〜12 ヵ月が 3 例であった。B 群では 31 例中，生後 1 ヵ月まで

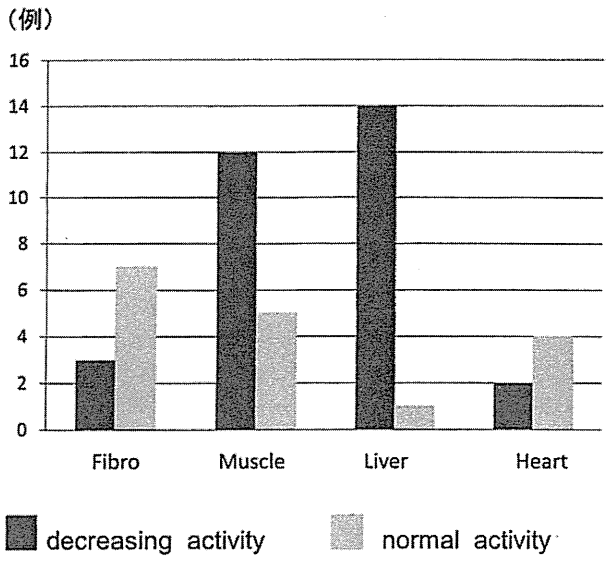

図7 A群における各臓器の酵素活性

の症状出現例が19例，1～3ヵ月が3例，4～12ヵ月が6例と1歳までに9割が症状出現していた。消化器症状の出現は両群ともに新生児期発症が過半数を占めていた。

3．臨床診断について

A群，B群の臨床診断を図5に示す。A群ではミトコンドリア心筋症を除き，どの臨床診断もほぼ一定数認められたのに対して，B群では致死型，非致死型乳児ミトコンドリア病，ミトコンドリア肝症の頻度が高かった。また，MRCD全体の臨床診断からみた場合に，乳児ミトコンドリア病，ミトコンドリア肝症において消化器症状が主症状で認められる頻度は高かった。

4．酵素診断および診断に至った試料について

臓器症状としての消化器症状が主であったA群25例の酵素診断結果を図6に示す。MRCD全体の酵素診断結果と異なり，複数の呼吸鎖複合体欠損が最多でほぼ半数の12例，次いでComplex Ⅰ欠損症7例，Complex Ⅳ欠損症4例，Complex Ⅲ欠損症2例であった。複数の呼吸鎖複合体欠損症の中にミトコンドリアDNA枯渇症候群2例が含まれていた。

各臓器毎の酵素活性の結果を図7に示す。主に筋肉，肝での酵素活性測定の結果，診断に至っており，筋肉において17例中12例，肝において15例中14例に酵素活性低下を認めた。線維芽細胞と心筋では，正常酵素活性が多くみられた。

考　察

MRCDにおける消化器病名として，難治性下痢症，嘔吐症，胃食道逆流症は頻度の高い重要な消化器病名であると考えられた。この中で，嘔吐症には胆汁性嘔吐が多く含まれており，これはpseudo-obstructionに似たメカニズムによる可能性がある。pseudo-obstructionは，臨床的に腸閉塞症と診断される症例において，開腹所見が正常の腸管の所見を呈する疾患である。Carlo[6]は，小児におけるpseudo-obstructionの原因としてウイルス感染（サイトメガロウイルス，ヘルペスウイルス，Epstain-Barrウイルスなど），胎児性アルコール症候群，MNGIEを含むミトコンドリア異常症をあげており，ミトコンドリア異常症では，消化管の吸収，分泌機能障害よりも運動機能障害が多い傾向にあると述べている。MNGIEでは，十二指腸の機械的閉塞が強く疑われ開腹手術となった症例で，術中に明らかな閉塞が認められなかった報告[7]があるが，我々の症例の中にも，頑固な胆汁嘔吐が持続し，消化管閉鎖が疑われて開腹手術となり，術中所見では消化管の機械的閉塞を認めずに後にMRCDの診断に至った症例も認められた。難治性下痢症では，分泌性下痢症[8]，短腸症候群[9]，吸収不良症候群，好酸球性胃腸炎など臨床診断は様々であった。胃食道逆流は，検査で確定された症例や臨床診断された症例を含むが，頻回嘔吐として経過をみられている症例の中には多数含まれている可能性がある。MRCDの診断に際しては，呼吸鎖複合体の中で最も不安定であるのはComplex Ⅱであり，二次的に呼吸鎖活性が低下する場合はComplex Ⅱを中心に活性が低下してくることが知られており[10]，各複合体の活性を比較することによりMRCDによる一次的な低下かその他の疾患による二次的な活性低下であるかを判断し最終診断としている。

今回我々は，MRCDにおいて認められる消化器症状として①哺乳不良（嘔吐以外の原因による経口摂取不良）・嚥下障害，②嘔気・嘔吐，③下痢，④腹痛・腹部膨満・通過障害の4つに分類できた。それぞれの考えられる原因として，①では咀嚼筋などの筋力低下，歯列不整，アカラシア，脳幹症状，小脳症状，②では胃不全麻痺（gastroparesis），pseudo-obstruction，腸管運動機能障害（dysmotility），脳幹・脊髄症状，前庭神経症状，③では，腸管運動障害，絨毛萎縮，膵外分泌機能障害，吸収不良，④では腸管運動障害の他，腸炎・憩室炎などが考えられるなど，MRCDで認め